Reviewed Preprint
v1 • June 17, 2026
Not revised

For correspondence:
kirstin.gutekunst@uni-kassel.de

§ Shared first authorship

Competing interests: No competing interests declared

Funding: See page 25

Reviewing editor: Caetano Antunes, University of Kansas, United States

Story about honest mistakes: The cyanobacterium *Synechocystis* has a promiscuous Entner-Doudoroff (ED) aldolase but no functional ED pathway

Ravi Shankar Ojha[1,§], Marius Theune[2,3,§], Ruben Fritsche[2], Alexander Makowka[3], Marko Boehm[2,3], Carmen Peraglie[1], Christopher Bräsen[1], Jacky L Snoep[4,5], Martin Hagemann[6], Bettina Siebers[1], Kirstin Gutekunst[2,3]

[1]Molecular Enzyme Technology and Biochemistry (MEB), Environmental Microbiology and Biotechnology (EMB), Centre for Water and Environmental Research (CWE), Faculty of Chemistry, University of Duisburg-Essen, Essen, Germany • [2]Molecular Plant Physiology, Bioenergetics in Photoautotrophs, University of Kassel, Kassel, Germany • [3]Physiology and Biotechnology of the Plant Cell, Christian-Albrechts-University, Kiel, Germany • [4]Biochemistry, University of Stellenbosch, Stellenbosch, South Africa • [5]Molecular Cell Biology, Vrije Universiteit Amsterdam, Amsterdam, Netherlands • [6]Plant Physiology, University Rostock, Rostock, Germany

eLife Assessment

This study presents **fundamental** results on the presence of the Entner-Doudoroff pathway in cyanobacteria. In contrast to an earlier study, **compelling** evidence is given that Synechocystis PCC 6803 lacks both an Entner-Doudoroff pathway and a related bypass but contains a promiscuous aldolase. This study successfully reconciles data from different studies and lessons learned from a previous misconception.

https://doi.org/10.7554/eLife.111485.1.sa3

Abstract

In 2016, the glycolytic Entner-Doudoroff (ED) pathway was reported in cyanobacteria and plants (1). The claim was based on the biochemical characterization of its key enzyme the 2-keto-3-deoxy-6-phosphogluconate (KDPG) aldolase EDA (ED aldolase), on protein sequence alignments, physiological data from cyanobacterial mutants, and the *in vivo* detection of an ED pathway specific metabolite (1). However, two enzymes 6-phoshogluconate (6PG) dehydratase (EDD) and EDA are unique to this route. A recent study suggests that EDD (Slr0452) from *Synechocystis* sp. PCC 6803 most likely encodes an enzyme involved exclusively in amino acid synthesis, indicating that a complete ED pathway would be missing (2). To answer the presence or absence of the ED pathway in *Synechocystis*, we conducted extended biochemical and physiological studies, revisited old data and resolved contradictions. These investigations reveal that *Synechocystis* lacks both an ED pathway and a glucose dehydrogenase/glucokinase (GDH/GK) bypass but contains a promiscuous aldolase EDA. EDA prefers KDPG as substrate but also decarboxylates oxaloacetate (OAA) and cleaves 2-keto-4-hydroxyglutarate (KHG). Synthesis of KDPG from pyruvate and glyceraldehyde 3-phosphate (GAP) is catalyzed with very low efficiency. These *in vitro* data suggest that EDA might be involved in the phosphoenolpyruvate (PEP)-pyruvate-OAA node and proline catabolism, which requires further clarification. The previous misconception was based on missing enzymatic characterizations, the oversight of a secondary mutation in a deletion strain, and an outdated view on carbohydrate fluxes. We conclude with a list of lessons and provide a solid foundation for future investigations into the role of EDA in cyanobacteria and other photoautotrophs.

Significance statement

This study provides a retrospective on why, for many years, it was mistakenly assumed that the glycolytic Enter-Doudoroff (ED) pathway exists in the cyanobacterium *Synechocystis* sp. PCC 6803. It shows that the first enzyme of this pathway, ED dehydratase EDD, is absent, while the second enzyme, 2-keto-3-deoxy-6-phosphogluconate (KDPG) aldolase EDA, is present but is promiscuous, cleaving KDPG in addition to 2-keto-4-hydroxyglutarate (KHG) and decarboxylating oxaloacetate (OAA) *in vitro*. Finally, valuable lessons are drawn from prior misconceptions and experimental limitations. This study provides a solid foundation for future studies on the role of the ED aldolase in absence of the ED pathway in cyanobacteria and other photoautotrophs.

Introduction

The carbon metabolism of cyanobacteria includes anabolic processes that build carbohydrates, like the Calvin-Benson-Bassham (CBB) cycle, as well as catabolic processes such as glycolytic pathways, in which these carbohydrates are consumed to provide intermediates, energy and reducing equivalents. In the day-night rhythm, carbohydrate fluxes alternate between anabolic and catabolic directions. In 2016, it was claimed that cyanobacteria and plants possess the Entner-Doudoroff (ED) pathway as a glycolytic route besides glycolysis (also known as Emden-Meyerhof-Parnas (EMP) pathway) and the oxidative pentose phosphate (OPP) pathway (Fig. 1A) (1). The ED pathway utilizes two enzymes that are unique to this route. The first enzyme is 6-phosphogluconate (6PG) dehydratase, abbreviated as EDD (ED dehydratase), which converts 6PG to 2-keto-3-deoxy-6-phosphogluconate (KDPG). The second enzyme is KDPG aldolase, which abbreviated as EDA (ED aldolase), which splits KDPG into pyruvate and glyceraldehyde 3-phosphate (GAP). This claim was mainly based on the biochemical characterization of purified KDPG aldolases (EDAs) from the cyanobacterium *Synechocystis* sp. PCC 6803 (hereafter *Synechocystis*) and the plant *Hordeum vulgare*, in combination with protein sequence alignments, growth experiments with selected cyanobacterial glycolytic deletion mutants and the detection of gluconate and KDPG in *Synechocystis* and *H. vulgare*, from which KDPG is a metabolite that is indicative of an active ED pathway (1). In the following years, *Synechocystis* mutants in which EDA was deleted either alone or in combination with other glycolytic enzymes, such as 6PG dehydrogenase (GND), which belongs to the OPP pathway, were characterized in detail and yielded contradictory results (3–7). These observations raised the question whether EDA could be either a promiscuous aldolase or an enzyme with moonlighting functions (3). Slr0452 from *Synechocystis* and its homologues in plants were considered to be EDDs (1). This consideration was based on protein sequence alignments, and in addition on a report of a promiscuous dihydroxy acid dehydratase (DHAD) with gluconate dehydratase (GAD) activity in *Sulfolobus solfataricus* also discussing similarities between the two dehydratases DHAD and EDD (1, 8). However, a recent study reported that the assumed EDDs in cyanobacteria and plants are instead in most cases exclusively DHADs (2). DHADs are specifically involved in the synthesis of the branched amino acids valine, leucine and isoleucine. Accordingly, raising further questions about the presence of the ED pathway in cyanobacteria and plants.

The anabolic CBB cycle and the catabolic glycolytic EMP and OPP pathways share several enzymes, requiring a sophisticated regulation of metabolic routes. Under photomixotrophic conditions, organic carbon (e.g., glucose) is consumed from the medium and metabolized in parallel with CO_2 fixation, accelerating growth compared to photoautotrophic conditions (9). It was previously observed that growth of the *Synechocystis* mutant Δ*pfk*Δ*zwf* in which the EMP and the OPP pathway were interrupted by deleting both phosphofructokinases (*pfk-A1* and *pfk-A2*) and glucose-6-phosphate dehydrogenase (*zwf*), was still able to enhance its growth in the presence of glucose (see Fig. 1) (1). This suggested the presence of an alternative route for carbohydrate degradation. When bioinformatic protein sequence analyses revealed the presence of both enzymes that are unique to the glycolytic ED pathway: EDD (Slr0452) and the KDPG aldolase EDA (Sll0107), this contradiction seemed to be resolved. EDA was purified and verified biochemically as KDPG aldolase (1). In addition, two putative glucose dehydrogenases (GDHs) (Sll1709 and Slr1608)

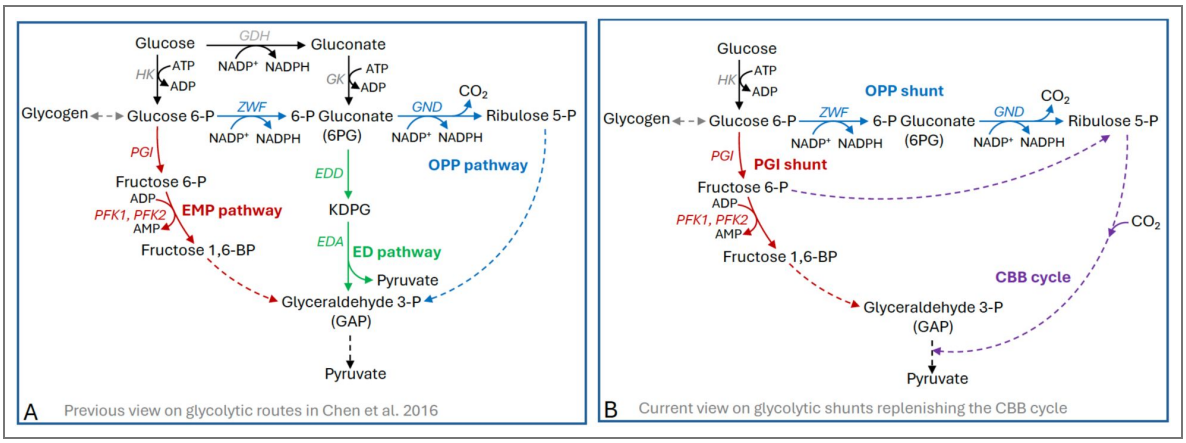

Figure 1. Previous and current view on glycolytic routes, glycolytic shunts and the CBB cycle in *Synechocystis*

(A) The central carbohydrate metabolism in *Synechocystis* as described by Chen et al (1). The shown GDH/GK bypass and ED pathway were assumed to be present based on the misinterpretation of experimental data (1). It was unclear at that time how glycolytic routes and the CBB cycle are organized under photomixotrophic conditions on glucose in continuous light. (B) Updated view where glycolytic routes and the CBB cycle are intertwined under photomixotrophic conditions so that glucose is fed via the glycolytic PGI and OPP shunt into the CBB cycle based on flux analyses (3). ED pathway and GDH/GK bypass are omitted based on results of this study. CBB, Calvin–Benson–Bassham; ED, Entner-Doudoroff; EDA, Entner-Doudoroff aldolase; EDD, Entner-Doudoroff dehydratase, EMP, Embden–Meyerhoff–Parnass; GDH, glucose dehydrogenase; GK, gluconate kinase; GND, 6-phosphogluconate dehydrogenase; HK, hexokinase; KDPG, 2-keto-3-deoxy-6-phosphogluconate; OPP, oxidative pentose phosphate; PFK, phosphofructokinase; PGI, phosphoglucose isomerase; ZWF, glucose-6-phosphate dehydrogenase.

were identified through bioinformatic studies. Since ZWF, which supplies the substrate 6PG for EDD, was deleted in Δ*pfk*Δ*zwf*, it was assumed that a putative GDH, together with a gluconate kinase (GK), would convert glucose (bypassing hexokinase (HK) and ZWF) to gluconate and further to 6PG (Fig. 1). Growth experiments with the respective deletion mutants seemed to support these assumptions (1). Furthermore, gluconate and KDPG were detected in cells of the *Synechocystis* wild type (WT) and Δ*pfk*Δ*zwf* via IC-ESI-MSMS (1). Hence, it was concluded that the accelerated growth of the Δ*pfk*Δ*zwf* mutant was made possible by the existence of a previously overlooked glycolytic ED pathway in combination with a GDH/GK bypass (1). Notably, at that time, it was not known whether the CBB cycle and glycolytic routes are spatially separated in the cytoplasm or rather intertwined with sophisticated regulation to enable a switch between anabolic and catabolic reactions. Subsequently, flux analyses with labelled glucose under photomixotrophic conditions with WT and Δ*eda* yielded interesting, but also contradictory results, as will be outlined in detail in the following (3). It was observed that glycolytic routes and the CBB cycle are highly intertwined in that sense that catabolic glycolytic routes are shortened to shunts that feed carbohydrates as anaplerotic reactions into the anabolic CBB cycle and thereby accelerate CO_2 fixation (3, 4). Two glycolytic shunts were identified: the OPP shunt, comprising the two first reactions of the OPP pathway catalyzed by ZWF and GND, and the PGI shunt, which includes only the first enzyme of the EMP pathway, phosphoglucose isomerase (PGI) (see Fig. 1) (3, 4). Whereas 27.6% of the labeled glucose was directed to the glycogen pool, the majority, 63.1%, was metabolized via the PGI shunt into the regenerative CBB cycle, and 9.3% were channeled via the OPP shunt to the CBB cycle (3). Contrary to our expectations, no flux via the ED pathway was detected, and no KDPG was measurable, despite the use of ultrasensitive LC–MS/MS.

The earlier assumption that the accelerated growth on glucose of the glycolytic Δ*pfk*Δ*zwf* mutant requires the GDH/GK bypass and the ED pathway, had been proven wrong by the described flux analyses, as this growth behavior can easily be explained by the existence of the PGI shunt which is responsible for the main flux of glucose into the CBB cycle and is still intact in the Δ*pfk*Δ*zwf* mutant (Fig. 1) (3). However, although there was no detectable flux via the ED pathway in the WT, carbohydrate fluxes were still altered in Δ*eda*. The flux via the PGI shunt was not modified, but a higher portion of labeled glucose was directed to the glycogen pool, and the flux through the OPP shunt was reduced (3, 4). Further studies yielded similarly conflicting results concerning the existence of the ED pathway and particularly concerning the phenotypes of Δ*eda* and the double mutant Δ*eda*Δ*gnd*. Both Δ*eda*Δ*gnd* and Δ*eda* were impaired in their ability to recover from nitrogen starvation, Δ*eda* had a reduced ability to respond to CO_2 shifts, the reactivation of the dark arrested CBB cycle was delayed and growth of mutants in which either *eda* was deleted alone or in combination with other glycolytic enzymes was not understandable on the mere interruption of glycolytic fluxes (4, 5, 7). Therefore, suggesting that alterations in Δ*eda* and Δ*eda*Δ*gnd* might rather be based on regulatory aspects such as a moonlighting functions or substrate promiscuity of EDA instead of missing fluxes (3). Enzymes with substrate promiscuity accept a broad range of substrates because their active sites can accommodate molecules with different shapes or chemical groups. Therefore, they catalyze several reactions in addition to the primary, most efficient one (10). Moonlighting enzymes, on the other hand, perform additional functions that are independent of the catalytic activity and active site of an enzyme, such as protein-protein interactions, regulation of gene expression, or binding to RNA or DNA as transcription factors (11).

The most puzzling contradiction that remained was the observation that the intermediate 6-P gluconate(6PG) accumulates only in Δ*eda*Δ*gnd* (where both 6PG effluxes should be interrupted in the case of an existing ED pathway) but neither in Δ*eda* nor in Δ*gnd* (see Fig. 1A) (4).

In order to understand previous results in detail against the background of contradictory data and the new bioinformatic information that EDD is absent in most cyanobacteria (2, 12), we went back to old data, purified and tested the putative EDD (Slr0452), checked the existence of the previously presumes GDH/GK bypass, performed a series of control measurements with different mutants and resolved the accumulation pattern of 6PG in deletion strains. A detailed biochemical characterization of the KDPG aldolase EDA (Sll0107) reveals its promiscuity and provides initial evidence for its possible role in the absence of EDD in the cyanobacterium *Synechocystis*.

Results

In vitro characterization of the predicted EDD/DHAD in *Synechocystis*

Based on the biochemical characterization of the KDPG aldolase EDA in *Synechocystis*, we had previously assumed that Slr0452 encodes for an enzyme that is involved in both amino acid synthesis as dihydroxy acid dehydratase (DHAD) and the ED pathway as EDD, as it was shown that the bifunctional DHAD (DHAD, IlvD/EDD superfamily) in the (hyper)thermophilic archaeon *Sulfolobus solfataricus*, also accepts D-gluconate - and to a lesser extent, galactonate - as alternative substrates in addition to its canonical role in branched-chain amino acid biosynthesis (8). Similarly, DHAD from *Rhizobium leguminosarum* bv. *trifolii* exhibits activity toward several C5 and C6 sugar acids, including gluconate, and DHAD from *Fontimonas thermophila* has been engineered to increase its gluconate-dehydration activity by an order of magnitude. Together, these observations underscore the intrinsic substrate promiscuity of IlvD enzymes in the IlvD/EDD superfamily.

However, although at least some DHADs exhibit activity toward gluconate (sugar acids), they have not been shown to accept 6-phosphogluconate (6PG)—the physiological substrate of EDD in the canonical ED pathway—from any organism. One possible explanation for this limited overlap in substrate specificity was proposed by Evans et al.(2), who suggested that gluconate, being smaller and unphosphorylated, may fit within the DHAD substrate-binding pocket normally occupied by dihydroxy-isovalerate. However, the lack of crystal structures of DHAD bound to dihydroxy-isovalerate or of EDD bound to 6PG precludes direct structural comparisons, leaving the precise geometric and electrostatic determinants of substrate discrimination between these enzymes unresolved. Of note, archaea like *S. solfataricus* utilizing modified, branched ED pathway versions involving the dehydration of gluconate to KDG, do not employ a DHAD but a dedicated gluconate dehydratase (GAD) (phylogenetically grouped within the enolase superfamily, specifically a subgroup related to the mandelate racemase/muconate lactonizing enzyme (MR/MLE)) to catalyse this conversion. This indicates that DHAD side activity alone might be insufficient to sustain physiologically relevant flux through the modified ED pathway. To date, there is no evidence that DHAD can functionally replace a bona fide GAD from the enolase superfamily in these organisms *in vivo*.

A recent study supposes that Slr0452 from *Synechocystis* which was assumed to be an EDD is an exclusive DHAD based on the biochemical characterization of its homolog in soybean (*Glycine max*) (2). Notably, organisms harboring both DHAD and EDD activity typically encode an additional IlvD/EDD superfamily gene, likely originating from gene duplication. Thus, the presence of only a single DHAD candidate in *Synechocystis* argues against an EDD function. DHAD activity was indeed shown for Slr0452 in another study, however, its potential activity toward 6PG as a substrate was not evaluated, leaving unresolved whether Slr0452 encodes a strict DHAD or a bifunctional DHAD/EDD enzyme (13). To address this question, the *slr0452* gene from *Synechocystis* was heterologously expressed in *E. coli* and recombinant protein was purified (Fig. S1). For comparison, a DHAD from the cyanobacterium *Synechococcus elongatus* was purified and assayed under identical conditions as a positive control (12) (Fig. S2). Enzymatic assays confirmed that Slr0452 catalyzes the dehydration of 2R-dihydroxyisovalerate (2R-DHIV) to 2-ketoisovalerate (KIV), consistent with DHAD function (Fig. S3A). Slr0452 exhibited a specific activity of 2.0 U mg^{-1}, whereas DHAD from *S. elongatus* showed 0.8 U mg^{-1} with 2R-DHIV as substrate (Fig. S3A).

To test for potential dual DHAD/EDD activity, Slr0452 was subsequently assayed using 6PG as substrate. A biochemically characterized EDD from *Caulobacter crescentus* (14) served as a positive control. Despite screening a range of divalent metal cofactors (Mg^{2+}, Mn^{2+}, Zn^{2+}, Co^{2+}, Cu^{2+}, and Fe^{2+}), no measurable activity toward 6PG was detected for Slr0452 under any tested condition (Fig. S3B). In contrast, EDD from *C. crescentus* displayed robust 6PG dehydratase activity as expected (Fig. S2, Fig. S3B). To evaluate the possibility of a modified ED pathway in *Synechocystis*,

Slr0452 and EDA (Sll0107) activities were also assayed using gluconate and KDG as substrates, respectively. *S. solfataricus* DHAD with GAD activity (*Sso*DHAD) and *Sulfolobus acidocaldarius* KD(P)G aldolase (*Saci*KD(P)GA), previously shown to catalyze reactions with gluconate and KDG, respectively (15, 16), were used as positive controls (Fig. S2, Fig. S4). Slr0452 and EDA from *Synechocystis* showed no activity on gluconate or KDG indicating that they are not involved in a modified ED pathway (Fig. S4).

Collectively, these results demonstrate that *slr0452* encodes a monofunctional, metal-dependent DHAD rather than an EDD or a bifunctional DHAD/EDD enzyme. This confirms that Slr0452 is exclusively involved in amino acid synthesis and does not catalyze the first reaction of the ED pathway as previously suggested by others (2, 13).

Above all, these results show that *Synechocystis* lacks a canonical 6-phosphogluconate (6PG) or gluconate dehydratase and therefore does not contain either the canonical or modified glycolytic ED pathway.

Testing for the existence of the previously presumed GDH/GK bypass

We furthermore tested for the existence of the previously presumed glucose dehydrogenase/gluconate kinase (GDH/GK) bypass as an alternative route to hexokinase and ZWF for gluconate and 6PG production. Two putative GDHs (Sll1709, Slr1608) were previously identified in the genome based on protein sequence alignments (1). Crude cell extracts were analyzed for GDH and GK activity; however, analysis of crude extracts from *Synechocystis* WT, Δ*zwf*, as well as a putative GDH1 (Sll1709) overexpression mutant *sll1709*:oe revealed no detectable GDH activity under either photoautotrophic no photomixotrophic conditions (Fig. S5, Fig. S6, Fig. 2A-B).

Unfortunately, we were not able to overexpress putative GDH2 (Slr1608). Δ*zwf* was tested on the assumption that the GDH/GK route, if existent, might be upregulated in this mutant. The *sll1709*:oe overexpression mutant was tested to ensure sufficient enzyme amounts. Cell crude extracts of Δ*zwf* and purified putative GDH1 (Sll1709) were furthermore tested for GDH activity in an *in vitro* enzyme assay (Fig. S6, Fig. 2B). In this analysis, the two quinones 2,3-dimethoxy-5-methyl-1,5-benzoquinone (DMB) and duroquinone (DQ) were also tested as electron acceptors in addition to $NADP^+$ and NAD^+ since some glucose dehydrogenases are known to reduce quinones instead of $NAD(P)^+$. No significant amount of GDH activity was detected for any tested electron acceptor in the GDH eluate, as well as in a cell extract of photomixotrophically grown Δ*zwf* (Fig. 2B). Taken together, these results indicate that GDH activity, which converts glucose to gluconate, is absent in *Synechocystis in vivo*. However, the inability to detect enzymatic activity is never a completely safe proof for its absence as the conditions might not have been chosen correctly, the enzyme activity might be below detection limits, or the purified enzyme might have lost its activity during purification. Furthermore, we were not able to purify and test the second putative GDH2 (Slr1608). Therefore, the second enzyme of the putative GDH/GK route was sought. The search for homologues of GK in the *Synechocystis* genome, using GKs from *Escherichia coli* and *Pseudomonas aeruginosa* as baits, was not successful. In line with the *in silico* analyses, no gluconate kinase activity was detectable in either crude cell extracts from WT or Δ*zwf* (Fig. 2C). These results furthermore strengthen the assumption that a GDH/GK bypass is absent in *Synechocystis*.

In order to further investigate if the GDH/GK bypass is absent from all cyanobacteria, we conducted a second blast (BlastP) analysis. Similarity thresholds were set at a query score > 30 %, an identity score > 30 % and an e-value < 1^{-10}. At these threshold settings we found 261 cyanobacteria that possess putative homologs of GKs from *Escherichia coli* and *Pseudomonas aeruginosa* (Table S1). We searched for homologs of GDHs in these 261 cyanobacteria next to *Synechocystis*. As baits the NAD^+-dependent GDH 1GCO from *Bacillus megaterium* and the quinone-dependent GDH from *Acinetobacter calcoaceticus* were used (17, 18). While the results again showed a rather poor similarity for both putative GDHs (Sll1709 and Slr1608) from *Synechocystis* and thereby confirmed the lack of GDH activity in enzyme tests, good homologies were found for

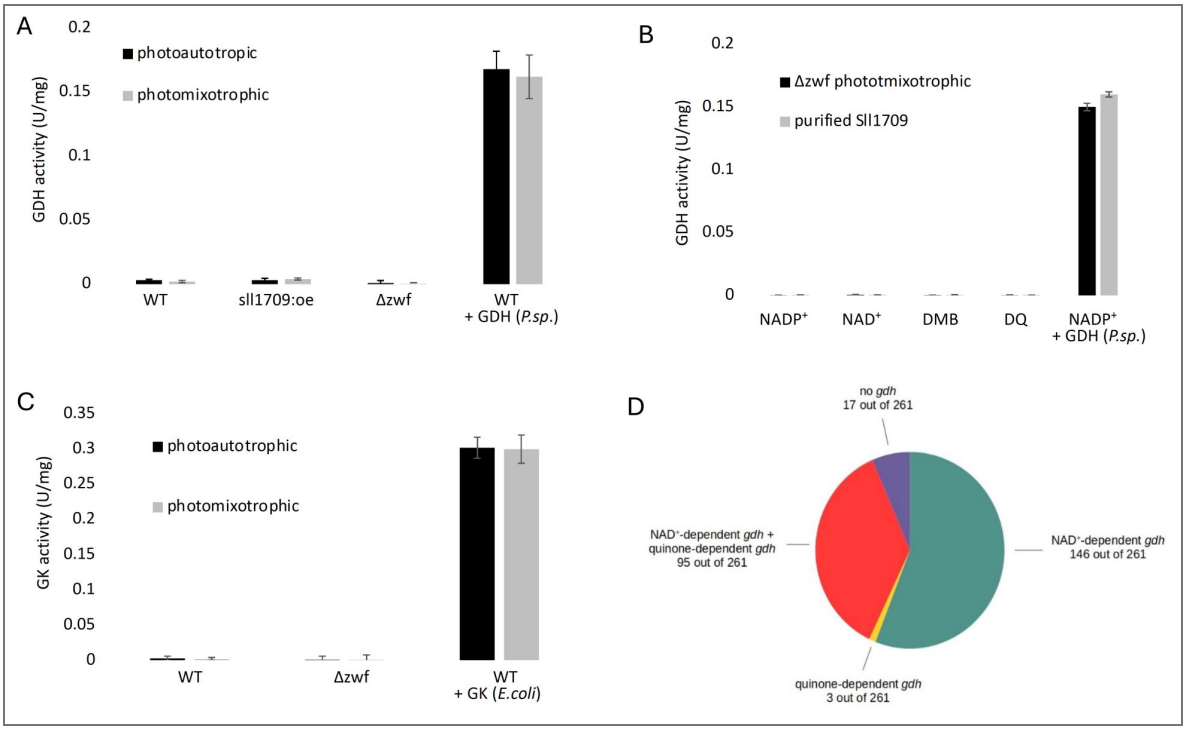

Figure 2. Evaluation of the proposed glucose dehydrogenase/gluconate kinase (GDH/GK) bypass in *Synechocystis* and representative cyanobacteria.

(A) GDH activity measurements in crude cell extracts of *Synechocystis* WT, Δ*zwf* and a strain overexpressing putative GDH1 (*sll1709*:oe) under photoautotrophic or photomixotrophic conditions. As a positive control, 0.05 U glucose dehydrogenase from *Pseudomonas sp.* was added to WT cell extract. (B) GDH activity measurements in crude cell extracts of photomixotrophically grown Δ*zwf* cultures and with purified putative GDH1 (Sll1709). $NADP^+$, NAD^+, and the two quinones DMB (2,6-Dimethoxy-1,4-benzochinon) and DQ (2,3-Dimethoxy-1,4-naphthochinon) were tested as electron acceptors. (C) Gluconate kinase activity measurements in cell extracts of *Synechocystis* WT and Δ*zwf* under photoauto-or photomixotrophic conditions. As a positive control, 0.05 U gluconate kinase from *E. coli* was added to WT cell extract. (D) Blast analyses of putative glucose dehydrogenase (GDH) in cyanobacteria. Protein databases of 261 cyanobacteria that also carry a putative gluconate kinase (GK) were analyzed for GDH homologues.

244 (93 %) of the other 261 analyzed cyanobacteria (Fig. 2D, Table S1). Out of these 244 cyanobacteria that possess both a putative GDH and a putative GK homologue, we picked two strains, namely *Spirulina sp. SIO3F2* and *Lyngbya aestuarii* and overexpressed and purified their putative GDHs (NEO87985.1 and WP_238987112) and the putative GK from *Lyngbya aestuarii* (WP_023068790.1) in *E. coli* (Fig. S7 to Fig. S9). Purification of the putative GK from *Spirulina sp. SIO3F2* (NEO86388.1 MAG) was not successful. Enzyme activity assays showed a clear GDH activity for both the GDH from *Spirulina* and the GDH from *Lyngbya* (Table 1). Both $NADP^+$ and NAD^+ could function as cofactors, while higher activity was observed with $NADP^+$ for both enzymes. The *Spirulina* and *Lyngbya* GDHs also used 2-Deoxy-D-glucose as substrate with 20-40% residual activity compared to glucose. Marginal activity with D-mannose was observed with the *Lyngbya* GDH (Table 1). All other tested substrates including fructose 6-phosphate, D-fucose, glucose 6-phosphate, lactose, D-glucosamine, D-lyxose, D-allose, D-arabinose, L-arabinose, D-xylose, L-xylose, and D-ribose were not used as substrates.

For both the GK from *Lyngbya* and *Spirulina,* expression in *E. coli* could be observed (Fig. S9), however, purification was only achieved for the GK from *Lyngbya.* For the Lyngbya GK a specific activity of 24.8 U/mg could be determined (Table 1). In combination with already shown GDH activity, this proves the presence of the GDH/GK bypass in this cyanobacterium.

Taken together, these results indicate that there is no GDH/GK bypass in *Synechochstis,* whereas it seems to be present in other cyanobacteria, as e.g. *Lyngbya.*

Based on these results, we currently have no explanation for the gluconate that was detected in previous IC-ESI-MSMS measurements in *Synechocystis* (1). Supplementation of the growth medium with gluconate did not enhance growth of the WT which furthermore supports the absence of a gluconate kinase or alternatively gluconate transport into the cells (Fig. 3A). An additional control was performed by testing photomixotrophic growth of a hexokinase mutant (Δ*hk*, *sll0539*) assuming that a GDH/GK bypass if present might be upregulated in this mutant.

Two enzymes (Sll0539 and Slr0329) were previously identified as glucose phosphorylating enzymes, with Sll0539 as the main contributor, while the deletion of Slr0329 did not affect on glucose uptake or photomixotrophic growth (19, 20). Therefore, only Δ*hk* (Δ*sll0539*) was studied (21).

Enzyme assays confirmed that the Δ*hk* mutant lost its ability to phosphorylate glucose (Fig. 3B). It was furthermore unable to metabolize glucose from the medium and to accelerate its growth (Fig. 3C-D). The described phenotypes could be complemented in Δ*hk::hk*. These data further support the assumption that a GDH/GK bypass is absent in *Synechocystis*, because it should allow glucose utilization in the absence of hexokinase (Hk, Sll0539) otherwise.

Investigation into the causes why 6PG accumulates in Δ*eda*Δ*gnd* in the absence of the ED pathway, but not in Δ*eda* or Δ*gnd*

As our data indicate that the GDH/GK bypass is not present in *Synechocystis*, the only known source for 6PG would be the reaction catalyzed by ZWF (see Fig. 1). Based on this assumption, the accumulation of 6PG in Δ*eda*Δ*gnd* in contrast to Δ*eda* and Δ*gnd* is unexpected in the absence of an existing ED pathway (see Fig. 1) (4). This pattern of 6PG enrichment had led to believe for many years, despite conflicting results, that there must be at least a small flux through the ED pathway in *Synechocystis* (4). So, to resolve this apparent contradiction, we attempted to resolve the origin of the 6PG accumulation pattern in Δ*eda*Δ*gnd,* Δ*eda* and Δ*gnd.*

In order to test if ZWF is responsible for 6PG production in Δ*eda*Δ*gnd,* this enzyme was deleted in addition resulting in the mutant Δ*eda*Δ*gnd*Δ*zwf*. 6PG accumulation was abolished in Δ*eda*Δ*gnd*Δ*zwf* as expected, indicating, that ZWF activity was responsible for 6PG production in Δ*eda*Δ*gnd* (Fig. 4A).

We subsequently tested ZWF activities in Δ*eda*Δ*gnd,* Δ*eda,* Δ*gnd* and Δ*zwf* as a control and found to our surprise that ZWF activity was completely lacking in Δ*gnd* (Fig. 4B). Sequencing of the *zwf* gene in Δ*gnd*, revealed an insertion of an adenine in position 399, which results in a premature

Table 1. Specific activities of the two cyanobacterial GDHs from *Spirulina* and *Lyngbya* and the gluconate kinase from *Lyngbya*.

Enzyme assays were performed after recombinant expression in *E. coli* and following purification.

Glucose dehydrogenase (GDH)	Activity (U/mg) with $NADP^+$	Activity (U/mg) with NAD^+
GDH (NEO87985.1) from *Spirulina* sp. SIO3F2	5.63 (Glucose) 2.12 (2-Deoxy-D-glucose)	0.15 (Glucose)
GDH (WP_238987112) from *Lyngbya aestuarii*	20.2 (Glucose) 4.04 (2-Deoxy-D-glucose) 0.26 (D-Mannose)	2.95 (Glucose)
Gluconat kinase (GK)	**Activity (U/mg) with ATP**	
GK (WP_023068790.1) from *Lyngbya aestuarii*	24.79 (10 mM Gluconate)	

Figure 3. Utilization of gluconate and glucose as carbon source for growth in WT, Δ*hk* (Δ*sll0539*), and Δ*hk*::*hk*.

(A) Growth of WT in the absence and presence of gluconate. (B) Hexokinase activity in WT and Δ*hk* with 10 mM glucose. (C) Photomixotrophic growth of WT, Δ*hk*, and Δ*hk*::*hk*. (D) Glucose concentration (%) in the growth medium after inoculation (day 0; 10 mM glucose) and on day 4 in WT, Δ*hk*, and Δ*hk*::*hk*.

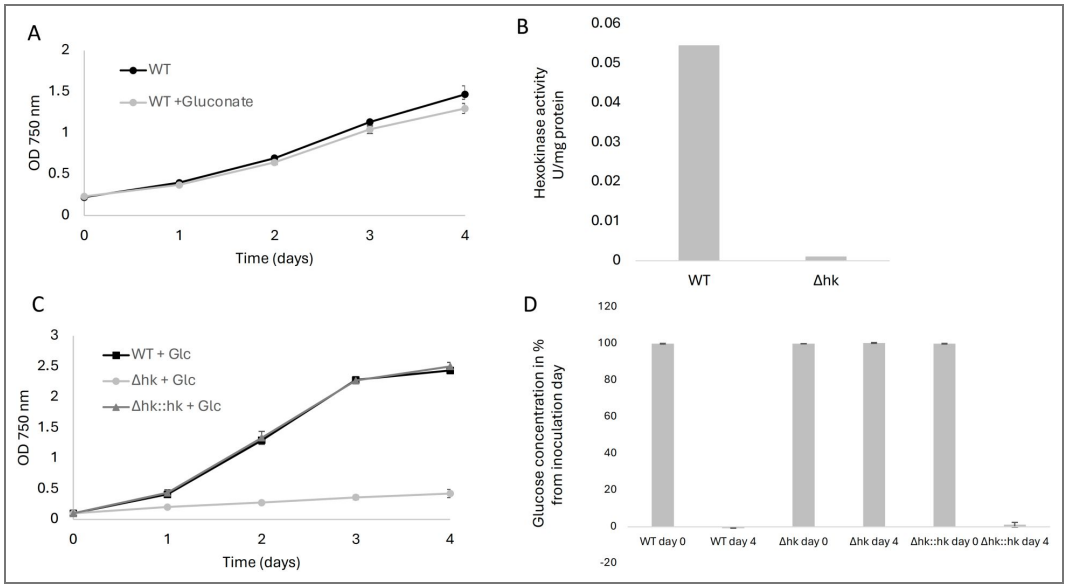

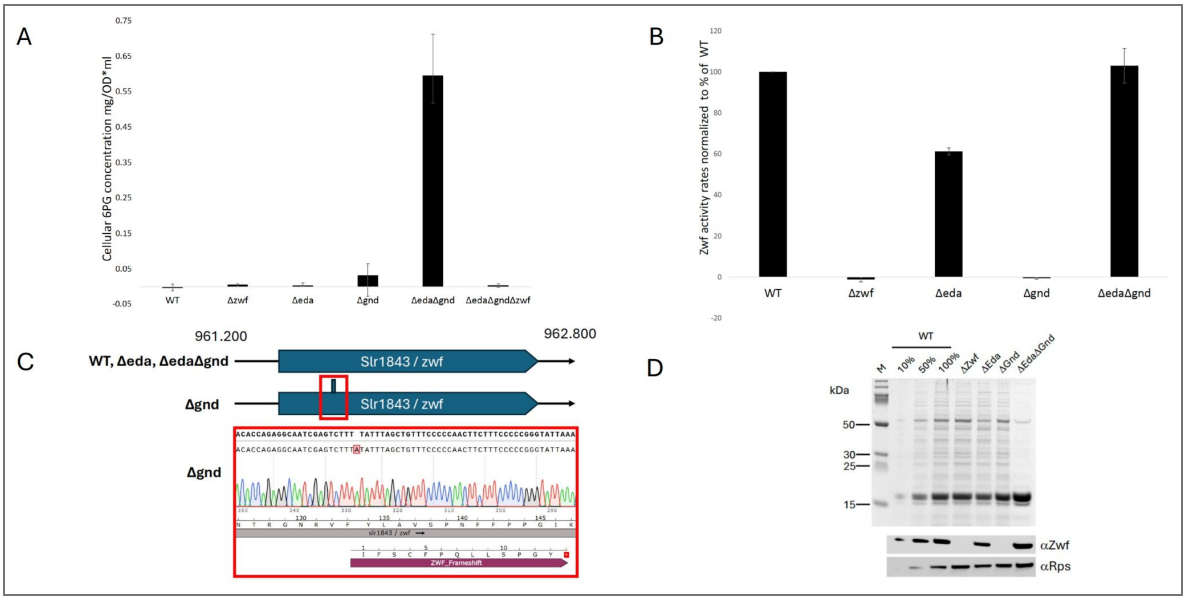

Figure 4. The accumulation of 6-phosphogluconate (6PG) in Δ*eda*Δ*gnd* in contrast to Δ*eda* and Δ*gnd* is not a result of a missing ED pathway flux but a secondary mutation in the *zwf* gene in Δ*gnd.*

(A) 6PG accumulation in WT, Δ*eda*Δ*gnd,* and Δ*eda*Δ*gnd*Δ*zwf* under photoautothrophic conditions. (B) Zwf activity measurements in cell crude extracts of WT, Δ*zwf*, Δ*gnd*, Δ*eda*, and Δ*eda*Δ*gnd.* reveals no Zwf activity in Δ*gnd.* The values are normalized to protein content. (C) Sequencing of the *zwf* genes of WT, Δ*gnd*, Δ*eda*, and Δ*eda*Δ*gnd* revealed the insertion of an adenine in position 399 in Δ*gnd,* which results in a premature stop codon. (D) Immunoblots of soluble cell extracts of WT, Δ*zwf*, Δ*gnd*, Δ*eda*, and Δ*eda*Δ*gnd* with antibodies specific against ZWF (αZwf). An antibody against 30S ribosomal protein (αRps) was utilized as a loading control. The WT was loaded in three different concentrations (10%, 50%, 100%) to facilitate relative quantification of the αZwf signals.

stop condon, and obviously completely abolishes ZWF activity in the Δ*gnd* mutant, whereas the mutants Δ*eda*Δ*gnd* and Δ*eda* lacked this insertion in their *zwf* genes (Fig. 4C). Immunoblots with specific antibodies against ZWF confirmed that ZWF is present in WT, Δ*eda* and Δ*eda*Δ*gnd* but is no longer expressed in Δ*gnd* (Fig. 4D). Whereas Δ*eda*Δ*gnd* showed ZWF activity that resembled or WT levels, ZWF activity was reduced to approximately 60% in Δ*eda* (Fig. 4B). This observation is in line with the reduced photomixotrophic flux through the OPP shunt in this mutant that we had observed earlier (3). The construction of corresponding complemented mutants (Δ*eda::eda*) is underway to test whether these differences are indeed due to the absence of EDA.

In summary, these data demonstrate that the accumulation pattern of 6PG in Δ*eda*Δ*gnd,* Δ*eda* and Δ*gnd* is not caused by an active ED pathway, as previously assumed. Instead, the pattern can be explained by a secondary mutation in *zwf* in the Δ*gnd* mutant which abolishes 6PG production in the Δ*gnd* mutant.

In vitro characterization of EDA (Sll0107)

Taken together, all data so far support the conclusion that the ED pathway is absent in the cyanobacterium *Synechocystis*. One remaining puzzling observation is the reported detection of KDPG in *Synechocystis* in one study using IC-ESI-MS/MS, which can be indicative of an active ED pathway, whereas another study using LC–MS/MS failed to detect this metabolite (1, 3). Analytical artifacts can never be fully excluded. To clarify whether EDA (Sll0107) might catalyze the reversible aldol condensation of pyruvate and GAP to KDPG, which could explain the detection of KDPG, in the absence of EDD and to test for potential promiscuity of EDA with several substrates, the *sll0107* gene (KEGG annotation) was expressed in *E. coli*. Although SDS–PAGE and Immunoblot blot analysis confirmed the expression of a ~23 kDa protein, it could not be eluted from the Ni–TED resin, and crude extracts lacked detectable KDPG aldolase activity. These observations suggested expression of a non-functional or truncated protein. Genomic inspection of *sll0107 (eda*) revealed an alternative start codon (genome position 2,972,167) 72 nucleotides upstream of the annotated start codon (genome position 2,972,095) (Fig. 5). Comparative sequence and AlphaFold 3 analyses (22) using *E. coli* and *C. crescentus* KDPG aldolases (23) as a reference, showed that only the upstream-initiated longer sequence retained the N-terminal α-helix characteristic of class I KDPG aldolases (Fig. 5A).

Therefore, the extended Sll0107 version was expressed in *E coli*, purified and resulted in active protein (Fig. S10-S12). SDS–PAGE showed a subunit mass of ~25 kDa, consistent with the calculated 23 kDa, and size-exclusion chromatography indicated a native mass of ~64 kDa, corresponding to a homotrimeric assembly typical of bacterial class I KDPG aldolases 13) (25, 26).

Biochemical enzyme characterization of Sll0107 (EDA)

Recombinant Sll0107 exhibited robust activity toward its canonical substrate KDPG, catalyzing its cleavage into pyruvate and GAP with a catalytic efficiency of 24.4 s^{-1} mM^{-1} (Fig. 6, Table 2). Inspired by recent reports that metal-independent class I KDPG aldolases from *Synechococcus elongatus* also accept oxaloacetate (12), we tested this substrate and found that EDA (Sll0107) catalyzed its cleavage to pyruvate and CO_2 with a catalytic efficiency of 0.58 s^{-1} mM^{-1} (Fig. 6, Table 2). Since elevated proline levels were previously reported in Δ*eda*, we next examined activity with 2-keto-4-hydroxyglutarate (KHG), an intermediate of the proline degradation pathway as substrate (5, 27). EDA efficiently cleaved KHG to pyruvate and glyoxylate with a catalytic efficiency of 0.18 s^{-1} mM^{-1} (Fig. 6, Table 2).

EDA exhibited a strong preference for KDPG as its primary substrate but also catalyzed reactions with OAA and KHG, albeit with substantially lower catalytic efficiency. The effect of $NADP^+$ on EDA activity was examined, as $NADP^+$ has been reported to act as an activator of *Synechococcus elongatus* EDA (12). Under the assay conditions used in this study, the addition of $NADP^+$ at concentrations up to 3 mM did not result in any measurable increase in EDA activity (Fig. 6E). These findings are consistent with curated enzyme data reported in BRENDA Enzyme Database (28), in which $NADP^+$ is not listed as an activator for EDA.

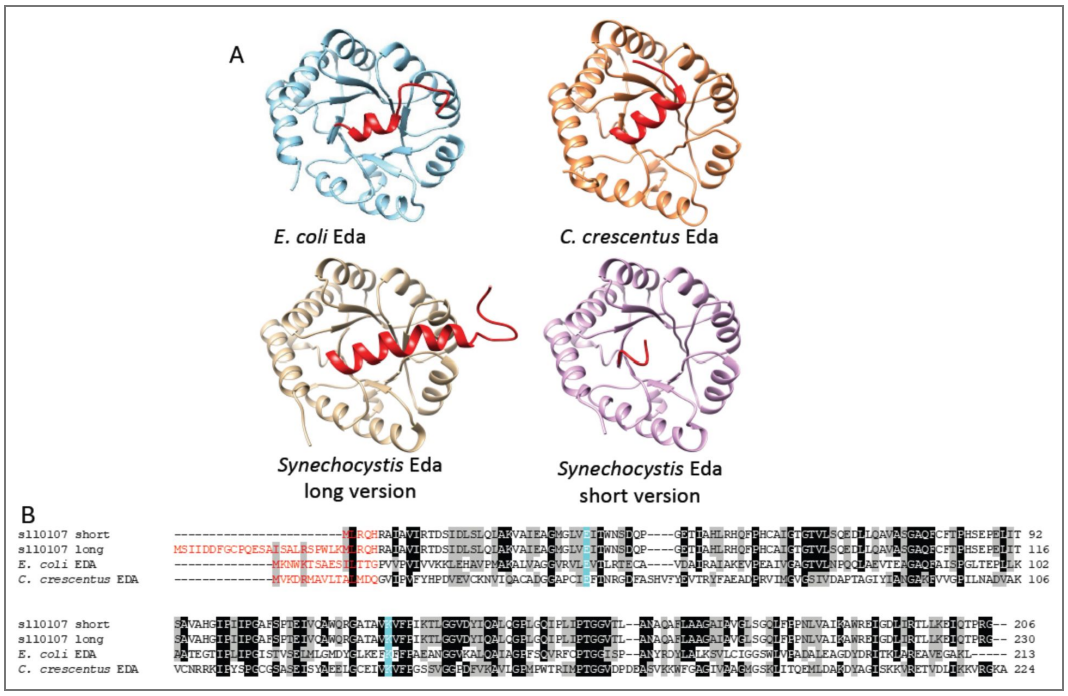

Figure 5. Structural comparison and sequence alignments of EDA enzymes including the genome-annotated version and an N-terminally extended version with an alternative start codon of the *Synechocystis* enzyme.

(A) Structures of *E. coli* and *C. crescentus* EDA enzymes are compared with AlphaFold 3 models of the N-terminally extended (long) and genome-annotated (short) *Synechocystis* EDA variants. The conserved N-terminal α-helix is highlighted in red. Amino acid sequences were retrieved from KEGG, AlphaFold 3 models were generated using AlphaFold Server v3.0 (22) and structures were visualized and edited using UCSF ChimeraX. (B) Sequence alignment highlighting the N-terminal residues of the conserved α-helix in red. The catalytic lysine responsible for Schiff-base formation and the glutamate acting as the acid/base catalyst are indicated in cyan. The alignment was performed using Clustal Omega (24) and manually visualized in BioEdit.

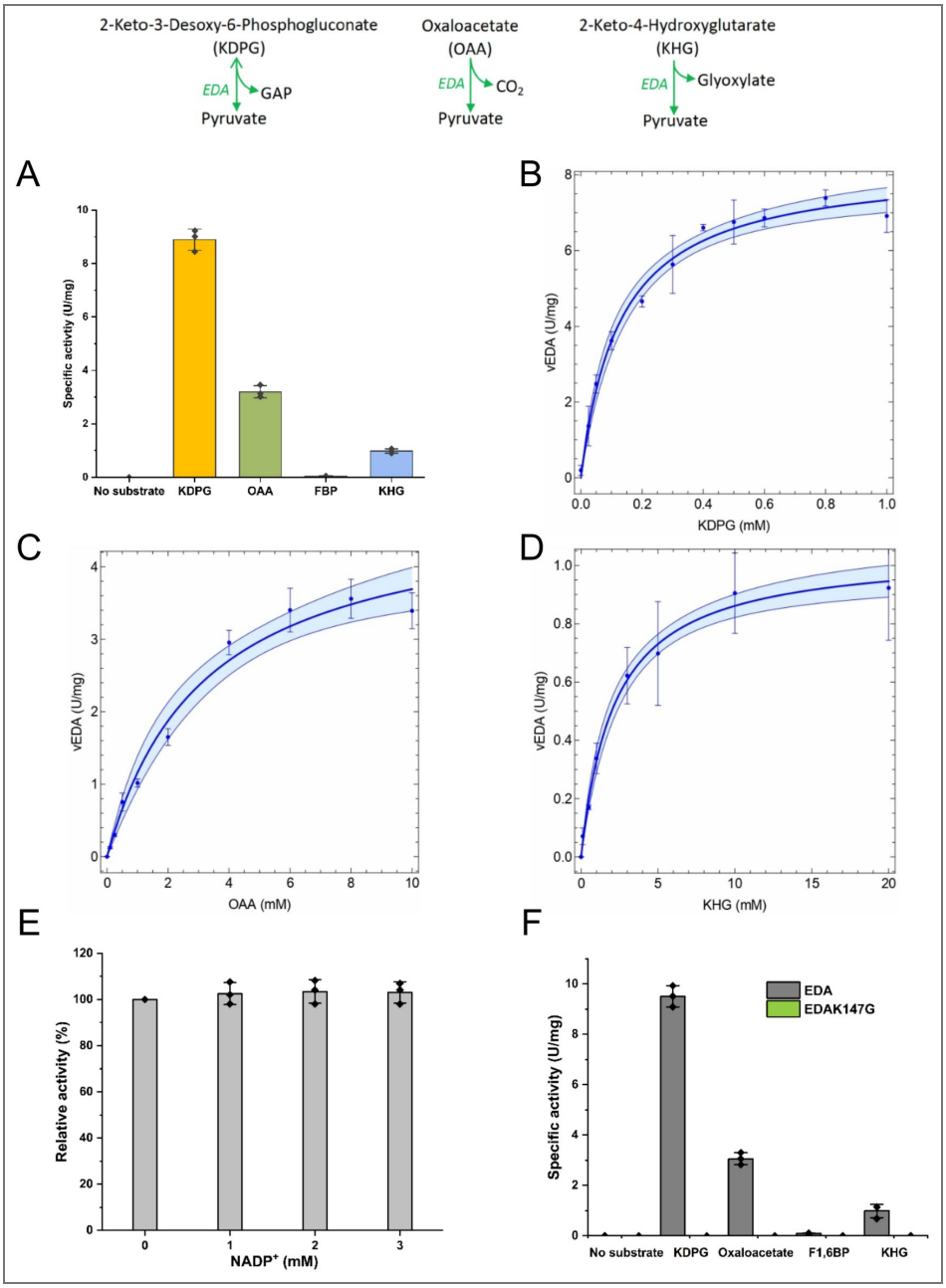

Figure 6. Substrate specificity and characterization of EDA (Sll0107) from *Synechocystis*.

(A) Substrate specificity was assessed with 5 mM of each KDPG, oxaloacetate, FBP, and KHG using the continuous coupled assay (see Methods). EDA exhibited high catalytic activity toward KDPG and reduced activity toward oxaloacetate and KHG, while no detectable cleavage of fructose 1,6-bisphosphate (FBP) was observed. This finding contrasts with the reported FBP cleavage activity of EDA from *Glycine max* (2). (B-D) Enzymatic characterization of EDA using KDPG, OAA and KHG as substrates. The activity of EDA was measured across a range of (B) KDPG, (C) OAA and (D) KHG concentrations (0–1 mM), (0-10 mM) and (0-20 mM) respectively. Colored bands indicate 95% confidence and data are shown as mean ± standard deviations from three technical replicates. The kinetic parameters of KDPG (V_{max} = 8.28 U mg^{-1}; K_m = 0.13 mM), OAA (V_{max} = 4.87 U mg^{-1}; K_m = 3.19 mM) and KHG (V_{max} = 1.05 U mg^{-1}; K_m = 2.18 mM) were determined by fitting the classical Michaelis–Menten equation using Wolfram Mathematica v14.2. (E) Effect of $NADP^+$ on EDA activity. Different $NADP^+$ concentrations (0, 1, 2 and 3 mM) were tested for their effect on EDA activity. Assays were performed with sub-saturating KDPG concentration (0.2 mM). The relative activity (%) in comparison to the control without effector (100%; specific activity of 4.3 U/mg) is shown. (F) Effect of K147G mutation on EDA activity. Enzymatic activity of wild-type EDA and the catalytic mutant EDAK147G was measured with 5 mM KDPG, oxaloacetate, FBP, and KHG using continuous coupled assays (see Methods). Data are presented as mean ± SD from three technical replicates (n = 3).

Substrates	V_{max}	K_m	k_{cat}	k_{cat}/K_m
KDPG	8.28 ± 0.25 U mg^{-1}	0.13 ± 0.01 mM	3.2 s^{-1}	24.4 s^{-1} mM^{-1}
OAA	4.87 ± 0.37 U mg^{-1}	3.19 ± 0.64 mM	1.86 s^{-1}	0.58 s^{-1} mM^{-1}
KHG	1.05 ± 0.03 U mg^{-1}	2.18 ± 0.24 mM	0.4 s^{-1}	0.18 s^{-1} mM^{-1}
FBP	No activity			
Malate	No activity			
Pyruvate + D-GAP	0.18 ± 0.01 U mg^{-1} (2.2% of the KDPG cleavage activity)			
Pyruvate + CO_2	No activity			
Pyruvate + glyoxylate	No activity			

Table 2. **Kinetic parameters of EDA (Sll0107) from *Synechocystis***

To assess reaction reversibility, a hallmark of class I aldolases, reported for archaeal KD(P)G aldolases (29), we tested the enzyme in the condensation direction using (i) pyruvate + GAP for KDPG formation, (ii) pyruvate + CO_2 for oxaloacetate, and (iii) pyruvate + glyoxylate for KHG synthesis. Only a low level of reverse activity, 0.18 U/mg (~2% of the cleavage activity) was detected for KDPG formation using a discontinuous TBA assay, whereas no reverse activity was observed for oxaloacetate or KHG synthesis (Fig. S12).

Given that a soybean KDPG aldolase was recently reported to accept fructose 1,6-bisphosphate (FBP) (2) we also tested FBP as a substrate. However, EDA (Sll0107) displayed no detectable activity with FBP (Fig. 6A, 6F, Table 2). Also, malate was not used as substrate (Table 2).

To confirm that catalysis proceeds via the conserved class I mechanism, the catalytic lysine in EDA was replaced by glycine through site-directed mutagenesis. The mutant enzyme EDAK147G was expressed and purified at comparable levels to the WT protein but exhibited no detectable activity with any tested substrate (Fig. 6F).

Taken together, these data show that the KDPG aldolase EDA (Sll0107) of *Synechocystis* is an aldolase with substrate promiscuity, which *in vitro* cleaves KDPG to GAP and pyruvate, OAA to CO_2 and pyruvate, and KHG to glyoxylate and pyruvate (Fig. 6, Table 2). In addition, it synthesizes KDPG from GAP and pyruvate with very low efficiency (~2% of the cleavage activity) (Fig. S12).

Since 6PG dehydratase (EDD) seems to be absent in *Synechocystis*, the canonical substrate of EDA, 2-keto-3-deoxy-6-phosphogluconate (KDPG) is not produced, and no alternative enzymatic source of KDPG is known to the best of our knowledge. Our *in vitro* enzyme assays therefore suggest that EDA may instead participate in alternative metabolic reactions, potentially linked to the PEP-pyruvate-OAA node and/or proline catabolism, as illustrated in Figure 7. However, further studies are required to clarify the physiological role of EDA *in vivo*.

Discussion

Our data demonstrate that *Synechocystis* lacks a functional ED pathway, due to the absence of both EDD and the proposed GDH/GK bypass, which is also supported by photomixotrophic flux analyses (3). Instead, it possesses a promiscuous EDA aldolase, whose physiological role remains to be elucidated. The dehydratases EDD and DHAD have a common origin, a high degree of amino acid and structural similarity, and the same catalytic mechanism, but differ in two domains that contribute to substrate selection, which is why EDD and DHAD are enzymes with high substrate specificity that cannot replace one another (2). Apart from four identified cyanobacteria identified as possessing potential EDDs (based on the described domains), most cyanobacteria lack EDD despite the presence of EDA, which likewise applies to algae, moss and plants (2, 27). Our data demonstrate that Slr0452 in *Synechocystis*, which we previously assumed as EDD (1), lacks 6PG dehydratase activity and instead dehydrates DIV exclusively, consistent with recent reports (13). The same experimental results were recently obtained for the cyanobacterium *Synechococcus* 7942 which also lacks EDD but contains EDA (12). This raises the question of what role EDA could play in the absence of EDD and the ED pathway in cyanobacteria, moss, algae and plants. In soybean (*Glycine max*), GmEDA was found to catalyze three reactions *in vitro*: firstly, the cleavage of KDPG to GAP and pyruvate, secondly the cleavage of fructose 1,6-bisphosphate (FBP) to dihydroxyacetone phosphate (DHAP) and GAP and thirdly the condensation of erythrose 4-phosphate (E4P) and GAP to sedoheptulose 1,7-bisphosphate (SBP) (2). Accordingly, the idea was put forward that GmEDA is a promiscuous aldolase which catalyzes aldolase reactions in the CBB cycle and glycolysis *in vivo*, which is well in line with its localization in chloroplasts (2). In diatoms the ED pathway was suggested to operate in mitochondria providing GAP and pyruvate to lower glycolysis and the TCA cycle, based on bioinformatic analyses, bacterial complementation experiments and measurements on the conversion of 6PG to pyruvate in soluble protein extracts (30–32). However, as neither the EDD nor EDA from diatoms were thoroughly characterized biochemically yet, further studies would be informative.

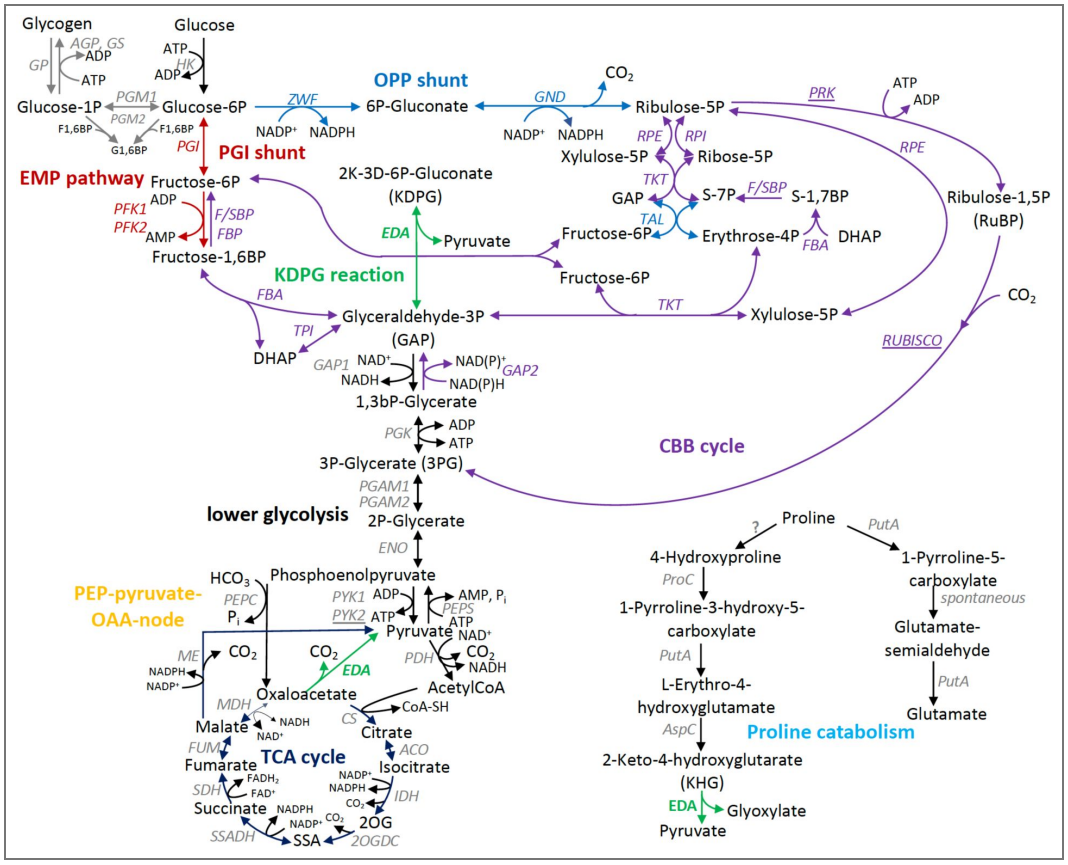

Figure 7. Proposed metabolic map of the central carbon metabolism in *Synechocystis* with all suggested *in vivo* roles of the promiscuous aldolase Sll0107 (EDA) highlighted in green, based on substrate promiscuity and activities observed *in vitro*.

ACO, Acontinase; AGP, ADP-glucose pyrophosphorylase; CBB, Calvin–Benson–Bassham; DHAP, dihydroxyacetone phosphate; E4P, erythrose 4-phosphate; EMP, Embden–Meyerhof–Parnas; EDA, Enter-Doudoroff aldolase; ENO, enolase; F6P, fructose 6-phosphate; FBA, fructose-bisphosphate-aldolase; FBP, fructose 1,6-bisphosphate; FBPase, fructose-1,6-bisphosphatase; F/SBPase, fructose-1,6-biphosphatase/sedoheptulose-1,7-biphosphatase; FUM, fumarase; GAP, glyceraldehyde 3-phosphate; GAPDH, glyceraldehyde-3-phosphate dehydrogenase; GBP, glucose 1,6-bisphosphate; GND, 6-phosphogluconate dehydrogenase; GP, glycogen phosphorylase; GS, glycogen synthase; HK, hexokinase; IDH, isocitrate dehydrogenase; ME, malic enzyme, MDH, malate dehydrogenase; OPP, oxidative pentose phosphate; PDH, pyruvate dehydrogenase complex, PEPC, phosphoenolpyruvate carboxylase, PEPS, phosphoenolpyruvate synthetase, PFK, phosphofructokinase; PGAM, phosphoglycerate mutase; PGI, phosphoglucose isomerase; PGK, phosphoglycerate kinase; PGL, 6-phosphogluconolactonase; PGM, phosphoglucomutase; PRK, phosphoribulokinase; PUTA, proline dehydrogenase; PYK, pyruvate kinase; R-5P, ribose 5-phosphate; RPE, ribulose-5-phosphate epimerase; RPI, ribose-5-phosphate isomerase; SDH, succinate dehydrogenase; TalB, transaldolase; TKT, transketolase; TPI, triosephosphate isomerase; X-5P, xylulose 5-phosphate; ZWF, glucose-6-phosphate dehydrogenase.

Based on our *in vitro* data *Synechocystis* EDA might be connected to the TCA cycle and the PEP-pyruvate-OAA node by decarboxylating oxaloacetate to pyruvate and in proline catabolism by splitting KHG to glyoxylate and pyruvate. The latter assumption is supported by earlier findings of elevated proline levels in Δ*eda* mutants of *Synechocystis* (5). For EDA from *Synechococcus* 7942, it has also recently been demonstrated that, in addition to cleaving KDPG, it also decarboxylates oxaloacetate (12). The catalytic efficiency of EDA on oxaloacetate is rather low (k_{cat}/K_m (mM^{-1} s^{-1}): 0.437) in *Synechococcus*, however, its activity could be enhanced by $NADP^+$. The *Synechocystis* EDA showed a 42-fold higher catalytic efficiency with KDPG compared to oxaloacetate (KDPG 24.4 s^{-1} mM^{-1}, OAA 0.58 s^{-1} mM^{-1}) and no activation by $NADP^+$ (1-3 mM) was observed. As the *Synechococcus* Δ*eda* mutant was compromised in terms of photosynthesis and growth under diurnal day/night cycles, the authors hypothesized that *Synechococcus* EDA might play a role in balancing NADPH/$NADP^+$ ratios and photosynthesis by modulating TCA cycle activities (12). For *Synechocystis* EDA, the catalytic efficiency for KDPG compared to KHG was 136-fold higher (KDPG 24.4 s^{-1} mM^{-1}, KHG 0.18 s^{-1} mM^{-1}). However, EDA displayed no detectable activity with FBP (Fig. 6), which is consistent with the fact that class I KDPG aldolases are members of a different enzyme class (EC 4.1.2.14). Likewise, class I and class II FBP aldolases (EC 4.1.2.13) are not known to exhibit activity toward KDPG (26, 33, 34). Interestingly, EDA was able to condensate GAP and pyruvate to KDPG *in vitro* with low efficiency. It remains to be tested whether this reaction could play a role *in vivo*, in which KDPG could act as a regulatory metabolite at low concentrations. This could explain why KDPG was detected in WT and Δ*pfk*Δ*zwf* in one study (1), although this observation could not be replicated later (3). Based on the current data, it is not possible determine whether the detected KDPG was due to a measurement artifact or not. The accumulation pattern of 6PG in WT, Δ*eda*, Δ*gnd* and Δ*eda*Δ*gnd*, which contradicted the flux analyses and had been interpreted as evidence of an active ED metabolic pathway in *Synechocystis* (3, 4), could be explained by a secondary mutation in the Δ*gnd* mutant (Fig. 4C) and now agrees with the flux analyses.

Our systematic re-examination of data on the proposed ED pathway in *Synechocystis* demonstrates how complementary approaches can contribute to elucidating cyanobacterial metabolism. By combining detailed biochemical enzyme characterization, genetic deletion and complementation, careful mutant validation, and taking into account metabolic flux analyses (3), we were able to clarify that neither EDD nor the GDH/GK bypass is present, and that the ED pathway is not functional in *Synechocystis*. These integrated studies further revealed the presence of a promiscuous KDPG aldolase whose broader metabolic involvement now opens exciting new research directions.

This study also highlights the importance of best practices to strengthen metabolic pathway reconstruction and provides the following lessons: Although protein sequence alignments provide valuable information, they cannot replace detailed biochemical enzyme tests, which are required to verify the predicted enzyme functions and to further test for substrate promiscuity. Furthermore, to demonstrate the presence of a metabolic pathway, it is advisable to characterize all enzymes of this pathway biochemically, rather than limiting analysis to individual key enzymes, and to also include flux analyses. Routine complementation of deletion mutants and sequencing of selected genes or the entire genome are effective means of identifying secondary mutations that can lead to misleading phenotypes. A final lesson is to exercise great caution when interpreting data and drawing conclusions, even if the data sets appear completely logical and conclusive at first glance (1). Over time, contradictory results have accumulated regarding the claim that there is an ED pathway in *Synechocystis*. In the present study, we have succeeded in clarifying a number of these contradictions. Taken together, these advances provide a solid foundation for future investigations into the *in vivo* role of the promiscuous aldolase EDA in cyanobacteria.

Materials and Methods

Growth experiments

Synechocystis sp PCC 6803 WT and mutants (Table S2) were grown in 200 ml BG11 medium (pH 8) in glass tubes at 28°C under constant light (50 µmol m^{-2} s^{-1}). Cultures were aerated with filter-sterilized air. Photomixotrophic cultures were supplemented with 10 mM D-glucose. Aliquots were taken under sterile conditions every 24 h to measure optical density photometrically at 750 nm.

Generation of mutants

Constructs for deletion mutants, complementation of Δhk and edaK147G were made by Gibson Assembly cloning, using the primers listed in Table S3. An antibiotic resistance cassette was fused to approximately 200 bp directly up- and downstream of the gene to be deleted and cloned into pBluescript. *Synechocystis* was transformed with these constructs to replace the gene with the antibiotic resistance cassette via homologous recombination. Mutants were checked via PCR for segregation.

Generation of a putative GDH1 (sll1709) His-tagged over-expression mutant (sll1709:oe) and overexpression of GDH homologues of Spirulina and Lyngbya

Two DNA fragments from the genome of *Synechocystis* were synthesized by Genescript: 1. a fragment containing 212 bp up- and 212 bp downstream of the s*ll1709* start codon, with a BamHI, XhoI and NdeI site in its middle and 20 bp of overlapping sequences with the pBluescript SK(+) vector at its ends (Fig. S5A). 2. a fragment containing a modified petE promotor, followed by His-tag, TEV cleavage recognition and linker encoding sequences, various restriction sites and 20 bp of overlapping sequences with the pBluescript SK(+) vector at its ends (Fig. S5B). Both fragments were separately cloned into the pBluescript SK(+) vector by Gibson Assembly cloning. A kanamycin antibiotic resistance cassette was inserted into the EcoRV site of the plasmid containing the modified petE promotor. Both plasmids were then digested with BamHI and NdeI and the promoter cassette was ligated into the alkaline phosphatase treated GDH1 plasmid to yield the final mutagenesis vector. This plasmid was transformed into *Synechocystis* and mutant segregation was confirmed by PCR analysis. GDH homologues of *Spirulina* and *Lyngbya* were overexpressed in *E.coli* (Fig. S7-8).

P3-His-GDH1 (sll1709) over-expression and His-tag purification

For the purification of GDH1 from *Synechocystis*, a 6 L photoautotrophic culture of the P3-His-GDH1 overexpression strain was grown to an OD_{750} of about 1. Cells were harvested by centrifugation at 4000 rpm in a JLA-8.1000 rotor for 20 min at 4°C. Initially, His-GDH1 over-expression in the 6 L culture was assessed by SDS PAGE analysis followed by immunoblotting with a His-tag specific antibody (Fig S6). A specific band could be detected in the over-expression mutant, confirming expression and stable accumulation of the over-expressed and N-terminally His-tagged GDH1 protein. A small-scale purification (using a 50-mL aliquot of the large culture) demonstrated that the protein could be purified (Fig S6C). For the large-scale purification the remaining cells were resuspended in lysis buffer (50 mM $NaPO_4$ pH=7.0; 250 mM NaCl; 1 tablet complete protease inhibitor EDTA free (Roche) per 50 mL) and broken by passing them through a French Press cell at 1250 p.s.i. twice. Unbroken cells and membranes were removed by centrifugation in a Beckman ultracentrifuge using a 70 Ti rotor at 30.000 rpm for 45 min at 4°C. The decanted soluble extract was adjusted to a volume of 45 mL with lysis buffer and incubated with 5 mL TALON cobalt resin (Takara) for 1 h at 4°C. The resin was then washed extensively with 200 mL lysis buffer and subsequently with 100 mL lysis buffer containing 5 mM imidazole. Bound proteins were eluted with 10 mL elution buffer (50 mM $NaPO_4$ pH=7.0; 250 mM NaCl; 250 mM imidazole) and after dialysis overnight against the reaction buffer 50 mM Tris pH=7.5; 20 mM MgCl, the protein was concentrated in a Vivaspin Turbo 4 Ultrafiltration Unit (5 kDa MWCO).

Commercially available Glucose dehydrogenase from *Pseudomonas* sp. (19359, Sigma) was resuspended in the reaction buffer for control measurements. Finally, protein concentrations were determined by Bradford assay using the Roti-Quant reagent (Carl Roth) and adjusted to 0.25 mg/mL. Samples taken during the purification procedure were assessed by SDS PAGE analysis followed by immunoblotting with antibodies specific against the His-tag.

Preparation of crude cell extracts

Enzyme activity was measured in crude cells extracts. For the generation of crude cell extracts of *Synechocystis*, an OD volume of 30-50 OD*mL sample culture was pelleted by centrifugation (5 min, 9000 *g*, 4 °C) and the pellet resuspended in 0.5 mL 100 mM Tris buffer (pH 7.6). The suspension was then transferred to centrifugation tubes with screwed lids (max 500 µl/cup) and glass beads (0.17-0.18 mm diameter; Sartorius, Göttingen, Germany) were added so that 1-2 mm liquid remained above the dispersion. Samples were vortexed for 10 min at 4 °C. Afterwards, the glass beads were pelleted by centrifugation in two consecutive centrifugation steps (1 min, 1000 *g*, 4 °C and 10 min, 1600 *g*, 4 °C). The supernatant was transferred to new centrifugation cups in between centrifugations. In order to precipitate cell debris, the supernatant was centrifuged (15 min, 18000 *g*, 4 °C) one more time. The supernatant constituted the final cell extract and was measured for its protein concentration and kept on ice until further enzyme activity measurements.

Protein quantification

Protein concentrations were determined according to Bradford (35). 1 µL protein sample (cell extract) was mixed in triplicates with 799 µL water. Afterwards, 200 µL Bradford reagent, consisting of 100 mg/L Coomassie Serva Blue G-250 (Bio-Rad, Munich, Germany), 5 % (v/v) ethanol and 8.5 % (v/v) H_3PO_4 was added to all samples as well as to 800 µL bovine serum albumin (BSA) standards in concentrations of 2, 5, 10, 15 and 20 µg/mL. After an incubation at RT for 10 min, absorption at 595 nm was measured and sample protein concentration calculated by using the standard curve.

Glucose dehydrogenase activity measurements

For glucose dehydrogenase (GDH) activity measurements in *Synechocystis*, NADPH turnover was monitored photometrically at 340 nm. Measurements were carried out in 50 µl crude cell extract or purified GDH in 100 mM Tris/HCl buffer (pH 7.4) in the presence of 20 mM glucose, 5 mM $NAD(P)^+$ and 10 mM $MgCl_2$. Reactions were started by addition of glucose. The kinetics of the reaction were monitored with a double-beam spectrophotometer for 5-10 minutes. In case quinones were tested as electron acceptors, the GDH reaction was enzymatically coupled to the gluconate kinase (GK) and 6PG dehydrogenase (GND) reaction, the latter providing the required $NADP^+$ turnover. This was achieved by adding 5 mM ATP, 0.02 U gluconate kinase from *E. coli* (Megazyme, Wicklow, Ireland) and 0.005 U 6-phosphogluconate dehydrogenase from *E. coli* (Megazyme, Wicklow, Ireland). The two tested quinones 2,3-dimethoxy-5-methyl-1,5-benzoquinone (DMB) and duroquinone (DQ) were supplied in a concentration of 5 mM. As a positive control, 0.05 U glucose dehydrogenase from *Pseudomonas sp.* (Sigma Aldrich, Steinheim, Germany) was added.

The GDH activity of recombinant enzymes from *Spirulina* sp. SIO3F2 and *Lyngbya* aestuarii was determined after GTS-His tag removal by TEV protease cleavage and purification. Activity was determined spectrophotometrically by monitoring glucose dependent reduction of $NAD(P)^+$ to NAD(P)H at 340 nm and 30°C (extinction coefficient of NAD(P)H=6.22 $mM^{-1}cm^{-1}$). The standard assay mixture (final volume of 500 µL) contained 0.1 mM Tris/HCl (pH 7.7 at 30°C), 10 mM $MgCl_2$, 5 mM $NAD(P)^+$, 20 mM Glucose, and 2.5 – 5 µg of recombinant protein. To determine the substrate specifity glucose was substituted by other sugars (for details see text).

Gluconate kinase activity measurements

For gluconate kinase (GK) activity measurements, the GK reaction was enzymatically coupled to the gluconate kinase (GK) and 6-phosphogluconate dehydrogenase (GND) reaction, the latter providing $NADP^+$ reduction, which was monitored photometrically at 340 nm. Measurements were carried out in 50 µl crude cell extract in 100 mM Tris buffer (pH 7.4) in the presence of 20 mM gluconate, 5 mM $NADP^+$, 10 mM $MgCl_2$., 5 mM ATP and 0.005 U 6-phosphogluconate dehydrogenase. Reactions were started by addition of gluconate and kinetics were monitored with a double-beam spectrophotometer for 5-10 minutes. As a positive control, 0.05 U gluconate kinase from *E. coli* (Megazyme, Wicklow, Ireland) was added.

Recombinant GK activity was determined spectrophotometrically in a continuous coupled pyruvate kinase/lactate dehydrogenase (PK/LDH) assay by monitoring NADH oxidation at 340 nm (30 °C) (extinction coefficient of NAD(P)H=6.22 $mM^{-1}cm^{-1}$). Gluconate phosphorylation was followed indirectly via ADP formation, which was converted by PK/LDH in a NADH-dependent reaction. The standard assay (500 µl) contained 100 mM Tris/HCL (pH 7.7), 10 mM MgCl2, 0.2 mM NADH, 1 mM PEP, 2 mM ATP, 1-10 mM gluconate, auxiliary enzymes PK and LDH, and 0.7-15µg purified recombinant enzyme (after GST-tag cleavage).

Glucokinase/hexokinase activity measurements

For glucokinase/hexokinase (GLK/HK) activity measurements, the GLK/HK reaction was enzymatically coupled to the glucose-6-phosphate dehydrogenase (ZWF) reaction, whose $NADP^+$ turnover was monitored photometrically at 340 nm. Measurements were carried out in 50 µl crude cell extract in 100 mM Tris buffer (pH 7.4) in the presence of 10 mM glucose or fructose, 5 mM $NADP^+$, 10 mM $MgCl_2$., 5 mM ATP and 0.005 U 6-phosphogluconate dehydrogenase from *E. coli* (Megazyme, Wicklow, Ireland). Reactions were started by addition of glucose and kinetics were monitored with a double-beam spectrophotometer for 5-10 minutes.

Quantification of 6-phosphogluconate

Quantification of 6-phosphogluconate (6PG) was achieved photometrically by enzymatic conversion of sample 6PG to ribulose-5-phosphate and CO_2, which goes hand in hand with equimolar formation of NADPH. 5 to 50 OD*mL cell culture was pelleted by centrifugation (5 min, 9000 g, 4 °C) and cell lysis was achieved by solving the pellet in 1 mL 0.2 M HCl, followed by a 15 min incubation at 95 °C. The lysates were centrifuged (10 min, 18000 g, 4°C) and the supernatants transferred to new tubes where they were neutralized by addition of 1 mL 1 M Tris/HCl buffer (pH 8.0). Samples were then split into two (each sub-pool 900 µL), that were supplied with 90 µL of an 11.11 mM $NADP^+$ solution. 10 µL of a 5 U/mL 6-PG dehydrogenase from (Megazyme, Wicklow, Ireland) solution was added to one of the samples, whereas 10 µL of water was added to the second sample as a control. All samples were then incubated at 37 °C for 30 min and the absorption at 340 nm was measured using a double-beam spectrophotometer. 6PG standards were prepared (0 mM, 0.05 mM, 0.1 mM, 0.2 mM, 0.4 mM and 0.8 mM) and measured in the same way as samples. Δabsorption values of standards were used to create a standard curve, which was then used to convert sample Δabsorption values into 6PG concentrations. The resulting 6PG concentration (mM) was converted into specific cellular 6PG content (µg/OD*mL) by multiplying it with the molar mass and dividing it by the respective OD volume.

Quantification of glucose

For quantification of medium glucose concentrations, 1 mL Synechocystis culture was pelleted by centrifugation (5 min, 10000 g, RT) and 50 µL of supernatant were transferred to a new cup. If medium glucose concentration was expected to exceed 5 mM, samples were diluted. 50 µL glucose standards with the following concentrations were prepared: 0 mM, 0.625 mM, 1.25 mM, 2.5 mM and 5 mM. Furthermore, a 'NADP buffer', containing 150 mM $NADP^+$, 150 mM ATP, 300 mM $MgCl_2$ in 100 mM Tris-HCl (pH 7.4,) was prepared. 940 µL 'NADP buffer' were added to all samples and standards, which were then transferred to acryl-cuvettes and absorption at 340 nm was measured

in a double-beam spectrophotometer (baseline absorption). After that, 0.17 U Hexokinase as well as 0.085 U glucose-6-phosphate dehydrogenase were added to all samples and standards. Samples and standards were then incubated at 37 °C for 60 min to ensure complete enzymatic conversion. Finally, absorption at 340 nm was measured again (endpoint absorption). Baseline absorbance values were subtracted from endpoint readings to calculate ΔA_{340}. A glucose standard curve was generated from the standards and used to determine glucose concentrations in the culture supernatants.

Blast analysis

In order to search for the existence of a gluconate kinase in the genome of *Synechocystis* and cyanobacteria in general, the fasta protein sequences of the well characterized gluconate kinases from *Escherichia coli* (KIG95398.1) and from *Pseudomonas aeruginosa* (WP134279162.1) were used as baits for the protein/protein blast tool at NCBI. Similarly, the fasta sequences of the NAD^+ dependent glucose dehydrogenase 1GCO from *Bacillus megaterium* and the quinone dependent glucose dehydrogenase 1C9U from *Acinetobacter calcoaceticus* were used as baits for the search of gluconate dehydrogenases in cyanobacteria. Next to *Synechocystis*, 261 cyanobacterial species were analyzed. Homology thresholds were set at a query score > 30 %, an identity score > 30 % and an e-value < 1^{-10}.

SDS PAGE and immunoblotting analyses

To assess the level of ZWF protein in various strains, soluble protein extracts were prepared and analysed by SDS PAGE and immunoblotting. 5 µg of protein were loaded per lane on a 12.5% (w/v) polyacrylamide BisTris gel using MES running buffer (250 mM MES, 250 mM Tris, 5 mM EDTA, 0.5 % (w/v) SDS). Gels were Coomassie-stained or electroblotted onto nitrocellulose membrane. For immunoblotting, 5% (w/v) milk powder in 1x PBS-T was used as blocking solution and all washing steps were performed with 1x PBS-T. For detection a ZWF antibody (αZwf, Agrisera, Sweden, Phyto AB, PHY5113A) in a 1:5k dilution in 1x PBS-T and a horseradish peroxidase-conjugated secondary antibody (anti-rabbit,1:10k in 1x PBS-T Cytiva) were used. As a loading control an antibody against 30S ribosomal protein S1 (αRps, Agrisera, Sweden) was utilized.

Gene cloning and protein overexpression

Codon-optimized genes from *Synechocystis* (*eda*, *sll0107*, *edd/dhad*, *slr0452*) and *Synechococcus elongatus* PCC 7942 (*dhad*, *syc0898c*) were synthesized by BioCat GmbH (Germany). The *dhad* gene from *Sulfolobus solfataricus* (*ss03107*), encoding a DHAD with GAD activity was synthesized by Eurofins (Eurofins Genomics, Ebersberg, Germany). A longer *sll0107* variant, extended by 24 amino acids relative to the KEGG annotation with an N-terminal 6×His tag was synthesized by BioCat GmbH (Germany) as well. The *slr0452* and *syc0898c* genes were inserted into pET24a vectors encoding a C-terminal 6×His-tag. The *saci_0225* gene from *Sulfolobus acidocaldarius* (encoding KDPG aldolase) was cloned into the pET15b vector using NdeI and BamHI restriction sites. Genes encoding *eda* (*ccna_01562*) and *edd* (*ccna_02134*) from *Caulobacter crescentus* were cloned into pET28b and pET15b using NdeI/BamHI and NdeI/HindIII, respectively. All constructs were verified by Sanger sequencing (LGC Genomics, Berlin, Germany). For protein expression, plasmids were transformed into *E. coli* Rosetta (DE3) (Agilent Technologies). Cultures were grown in Terrific Broth (TB; 22 g L^{-1} yeast extract, 12 g L^{-1} tryptone, 4 mL L^{-1} glycerol) supplemented with the appropriate antibiotics (100 µg mL^{-1} ampicillin or kanamycin, and 30 µg mL^{-1} chloramphenicol) at 37 °C with shaking at 180 rpm. Protein expression was induced at an OD_{600} of 0.6–0.8 by addition of 1 mM isopropyl-β-D-thiogalactopyranoside (IPTG), followed by incubation at 18 °C for 18–22 h. Cells were harvested by centrifugation (15 min, 8630 × *g*, 4 °C) and stored at −70 °C until further use.

EDA (KDPG aldolase) mutation at the active center

Class I KDPG aldolases are metal-independent enzymes that utilize a catalytic lysine residue to form a Schiff base intermediate during catalysis. In Eda this lysine (Lys147, based on the extended *sll0107* sequence) was identified as essential for activity toward multiple sugar acid substrates

(36). To generate a catalytically inactive variant, Lys147 was substituted with glycine (K147G), which lacks both side-chain and net charge. Site-directed mutagenesis was performed as described (37). Q5® High-Fidelity DNA Polymerase and its recommended reaction buffer (NEB) were utilized for the amplification process. The primers used for mutagenesis are listed in Table S3, with the nucleotide substitutions introducing the K147G exchange underlined. As a template the codon-optimized *eda* gene from *Synechocystis* (*sll0107*) that was synthesized by BioCat GmbH (Germany), was utilized. Successful mutagenesis was confirmed by DNA sequencing (LGC genomics, Berlin, Germany). The resulting EDA variant was named EDAK147G.

Protein purification

Recombinant *Synechocystis* EDA (both versions), EDAK147G, and DHAD (Slr0452), recombinant *Caulobacter crescentus* CcEDA and CcEDD, *Sulfolobus acidocaldarius Saci*KD(P)GA, and *Sulfolobus solfataricus SsoDHAD* were purified by immobilized metal affinity chromatography (IMAC) followed by size-exclusion chromatography (SEC) for EDA and Slr0452. Frozen cell pellets were resuspended in 50 mM HEPES–NaOH (pH 7.8, 30 °C), 300 mM NaCl at a ratio of 1 g wet cells per 3 mL buffer. For EDD/DHADs purification buffer was supplemented with 10 mM $MgCl_2$ and 1 mM DTT. Cells were disrupted by sonication (3 × 5 min; amplitude 50; cycle 0.5) using a UP200S homogenizer (Hielscher Ultrasonics, Brandenburg, Germany). Cell debris was removed by centrifugation (45 min, 21,130 × *g*, 4 °C). His-tagged proteins, except *Synechocystis* DHAD (Slr0452), were purified from the supernatant using Ni–TED columns (Macherey-Nagel, Düren, Germany) according to the manufacturer's protocol. *Synechocystis* DHAD (Slr0452) was purified on a self-packed Ni–NTA affinity column. Elution fractions containing the target protein were pooled and concentrated using Vivaspin 20 centrifugal concentrators (Sartorius Stedim Biotech; 30 kDa cutoff for EDD/DHAD and 3 kDa cutoff for EDA). Concentrated samples of *Synechocystis* EDA (6 mg protein) were further purified by SEC on a HiLoad 16/600 Superdex 200 prep grade column (Cytiva, Marlborough, MA, USA) equilibrated with 50 mM HEPES–NaOH (pH 7.8, 30 °C), 300 mM NaCl and additionally contained 10 mM $MgCl_2$ and 1 mM DTT for DHADs purification. Protein-containing fractions (4.5 mg after SEC) were analyzed by SDS–PAGE and enzymatic activity assays. Purified proteins were stored at −70 °C in 25% (v/v) glycerol. Protein concentrations were determined by the Bradford assay (38) using bovine serum albumin (Merck, Darmstadt, Germany) as the standard.

Determination of the native molecular mass of EDA

Following IMAC purification, 6 mg of purified EDA was subjected to SEC on a HiLoad 16/600 Superdex 200 prep-grade column (Cytiva, Marlborough, MA, USA). The column was calibrated under identical buffer conditions using standard proteins from the LMW and HMW gel-filtration calibration kits (Cytiva, Marlborough, MA, USA): Aprotinin (6.5 kDa), Ribonuclease A (13.7 kDa), Ovalbumin (44 kDa), Aldolase (158 kDa), and Ferritin (440 kDa), with blue dextran to determine the column void volume. The native molecular mass of EDA was estimated from the resulting calibration curve.

In vitro EDA enzyme characterization

The catalytic activities of *EDA*, EDAK147G, *Saci*KD(P)GA, and *Cc*EDA in the KDPG cleavage direction were determined using a continuous, coupled spectrophotometric assay. EDA catalyzes the cleavage of 2-keto-3-deoxy-6-phosphogluconate (KDPG) into pyruvate and glyceraldehyde 3-phosphate (GAP). Pyruvate formation was monitored indirectly by its reduction to lactate using lactate dehydrogenase (LDH; rabbit muscle, Merck, Darmstadt, Germany), coupled to the oxidation of NADH to NAD^+. The decrease in absorbance at 340 nm was recorded in 96-well plates (BRANDplates®, BRAND, Wertheim, Germany) using a Tecan Infinite M200 plate reader (Tecan Group AG, Männedorf, Switzerland) at 30 °C. NADH concentration was quantified against a standard curve ranging from 0–0.7 mM.

For KDPG cleavage assays (200 µL final volume), reactions contained 0.1 M HEPES–NaOH (pH 7.8, 30 °C), 0.7 mM NADH, 2 mM KDPG, 2 U LDH, and the indicated enzyme (typically 1 µg EDA, EDAK147G, *Saci*KD(P)GA, or 0.06 µg *Cc*EDA). Substrate specificity toward oxaloacetate (OAA) and 2-

keto-4-hydroxyglutarate (KHG) was assayed under the same conditions as KDPG assay, as they all generate pyruvate as one of the two product, however, for the KHG assay, 6 µg of EDA was used.

FBP cleavage activity forming GAP and DHAP was assayed using a coupled system containing glycerol-3-phosphate dehydrogenase (G3PDH; rabbit muscle, Merck, Darmstadt, Germany), which converts the DHAP product to glycerol 3-phosphate coupled to the oxidation of NADH to NAD^+. Reaction mixtures (200 µL) contained 0.1 M HEPES–NaOH (pH 7.8, 30 °C), 0.7 mM NADH, 5 mM FBP and 2 U G3PDH. FBP aldolase (from *Saccharomyces cervisiae*; Merck, Darsmstadt, Germany) served as the positive control. Reactions were initiated by addition of enzyme, and all measurements were performed in triplicate. Negative controls omitted either enzyme or substrate. To obtain the kinetic parameters (Table 1), a classical Michaelis-Menten rate equation was fit to the complete dataset using NonlinearModelFit function in Wolfram Mathematica v14.2. EDA activity in the reverse (condensation) direction—forming KDPG from pyruvate and D-GAP was quantified using the colorimetric thio-barbituric acid (TBA) assay as described (39). Reactions (1 mL) contained each 20 mM pyruvate and 10 mM D-GAP in 0.1 M HEPES–NaOH (pH 7.8, 30 °C) with 15 µg EDA or 3 µg *Saci*KD(P)GA, *Saci*KD(P)GA was assayed at 70°C. At two-minute intervals, 50 µL aliquots were quenched with 5 µL of 12% trichloroacetic acid. Absorbance of the TBA–KDPG adduct was measured at 549 nm (ε = 67.8 mM^{-1} cm^{-1}), and *Saci*KD(P)GA served as a positive control. EDA activity in reverse direction – forming OAA was assayed using malate dehydrogenase (MDH, *S. cervisiae*, Merck, Darmstadt, Germany) that forms malate from OAA by oxidation of NADPH to $NADP^+$. EDA activity in reverse direction – forming KHG from pyruvate and glyoxylate was assayed by measuring the pyruvate consumption in a discontinuous assay. Pyruvate (5 mM) and glyoxylate (5 mM) were incubated with Eda (5 µg) in in 1 mL of 0.1 M HEPES–NaOH buffer (pH 7.8) at 30 °C. At defined time points (0, 2, 4, 6, 8, 10, 20, and 30 min), 50 µL aliquots were withdrawn and quenched by the addition of 5 µL of 12% (v/v) TCA. Samples were immediately placed on ice and centrifuged at 8,130 × g for 10 min to remove precipitated protein. Supernatants (50 µL) were diluted into 950 µL of 0.1 M HEPES–NaOH (pH 7.8). Pyruvate consumption was quantified by a lactate dehydrogenase (LDH)–coupled assay using 0.7 mM NADH and 1 U of LDH (rabbit muscle; Merck, Darmstadt, Germany). The decrease in NADH absorbance reflected the conversion of pyruvate to lactate by LDH and was used to compare pyruvate levels across time points. It was ensured that auxiliary enzymes were not rate limiting. One unit (1 U) of enzyme activity is defined as 1 µmol substrate consumed or product formed per minute.

To test whether EDA exhibits activity toward 2-keto-3-deoxygluconate (KDG), an additional continuous coupled assay was employed. Reaction mixtures (200 µL final volume) contained 0.1 M HEPES–NaOH (pH 7.8, at 30 °C), 20 mM gluconate, 20 µg *Sulfolobus solfataricus* DHAD (*Sso*DHAD; SSO3107), 10 mM $MgCl_2$, and 1 mM DTT. The mixtures were incubated with 20 µg of either *Sso*DHAD at 50 °C or Slr0452 at 30 °C for 2 h. Reactions were initiated by the addition of EDA or *Sulfolobus acidocaldarius* KD(P)GA (*Saci*KD(P)GA; Saci_0225) as positive control, which converts the reaction product 2-keto-3-deoxygluconate (KDG) into pyruvate and glyceraldehyde. Pyruvate formation was detected as described above for the KDPG cleavage assay. All assays were performed in triplicate. Negative control reactions were performed in the absence of either the enzyme or the substrate.

In vitro EDD enzyme assay

EDD catalyzes the dehydration of 6PG to form KDPG in the classical Entner–Doudoroff pathway. Enzyme activity was monitored using a continuous, coupled spectrophotometric assay in which the KDPG product was subsequently cleaved by excess *Cc*EDA to yield pyruvate and GAP. Pyruvate formation was detected through its reduction to lactate by lactate dehydrogenase (LDH; rabbit muscle, Merck, Darmstadt, Germany), coupled to the oxidation of NADH to NAD^+. The decrease in absorbance at 340 nm was recorded in 96-well plates (BRANDplates®, BRAND, Wertheim, Germany) using a Tecan Infinite M200 plate reader (Tecan Group AG, Männedorf, Switzerland) at 30 °C. NADH concentrations were quantified against a standard calibration curve (0–0.7 mM). Reaction mixtures (200 µL final volume) contained 0.1 M HEPES–NaOH (pH 7.8, 30 °C), 0.7 mM NADH, 10 mM $MgCl_2$, 5 mM 6PG, 5 µg *CcEDA* (recombinantly produced and characterized in this

study, 150 U mg^{-1}), 2 U LDH, and the respective amounts of Slr0452 (20 µg) as the test sample and *Cc*EDD (5 µg) as positive control (40). Reactions were initiated by enzyme addition, and all assays were performed in triplicate. Negative controls omitted either the enzyme or substrate.

To test whether Slr0452 exhibits activity toward gluconate, as reported for the bifunctional EDD/DHAD from *Sulfolobus solfactorius* (15), an additional continuous coupled assay was employed. Reaction mixtures (200 µL final volume) contained 0.1 M HEPES–NaOH (pH 7.8, at 30 °C), 0.7 mM NADH, 10 mM $MgCl_2$, and 1 mM DTT. The mixtures were incubated with 20 µg of either *S. solfataricus* DHAD (*Sso*DHAD) at 50 °C or Slr0452 at 30 °C. Reactions were initiated by the addition of *Sulfolobus acidocaldarius* KD(P)GA aldolase, which converts the reaction product 2-keto-3-deoxygluconate (KDG) into pyruvate and glyceraldehyde (16). Pyruvate formation was detected as described above for the KDPG cleavage assay. All assays were performed at least in triplicate. Negative controls omitted either the enzyme or substrate. It was ensured that auxiliary enzymes were not rate limiting. One unit (1 U) of enzyme activity is defined as 1 µmol substrate consumed or product formed per minute.

In vitro DHAD enzyme assay

Dihydroxyacid dehydratase (DHAD; *ilvD*) catalyzes a key step in the biosynthesis of branched-chain amino acids (BCAAs: leucine, isoleucine, and valine). The activities of Slr0452 and *S. elongatus* DHAD (*Se*DHAD) were assayed using the physiological substrate 2R-dihydroxyisovalerate (DHIV; Merck, Darmstadt, Germany), which is dehydrated to yield 2-ketoisovalerate (KIV). Product formation was quantified using a discontinuous colorimetric assay as described previously (13).

Reaction mixtures (100 µL) contained 50 mM Tris–HCl (pH 7.8), 1 mM dithiothreitol (DTT), 10 mM $MgCl_2$, and 1 mM 2R-DHIV. Reactions were initiated by the addition of 0.25 µM enzyme, incubated aerobically at room temperature for 30 min, and terminated with 25 µL of 2 M HCl. The resulting KIV was derivatized by addition of 50 µL of saturated 2,4-dinitrophenylhydrazine (DNPH; Häberle, Germany) in 2 M HCl and incubated for 30 min at room temperature. Subsequently, 25 µL of 10 M NaOH were added, samples were mixed, and precipitates were removed by centrifugation (5,000 × *g*, 10 min). Supernatants (100 µL) were transferred to clear 96-well microplates, and absorbance of the KIV-DNPH adduct was measured at 540 nm. Quantification was based on a KIV-DNPH calibration curve (0–1 mM), which exhibited linear response across this range. All enzyme assays were performed in triplicate.

To test whether Slr0452 exhibits activity toward gluconate, as reported for the bifunctional DHAD from *Sulfolobus solfataricus*, (15) an additional continuous coupled assay was employed. Reaction mixtures (200 µL final volume) contained 0.1 M HEPES–NaOH (pH 7.8, at 30 °C), 20 mM gluconate, 10 mM $MgCl_2$, and 1 mM DTT. The mixtures were incubated with 20 µg of either *Sso*DHAD at 50 °C or Slr0452 at 30 °C. Reactions were initiated by the addition of *Saci*KD(P)GA, which converts the reaction product 2-keto-3-deoxygluconate (KDG) into pyruvate and glyceraldehyde (16). Pyruvate formation was detected as described above for the KDPG cleavage assay. All assays were performed in triplicate. Negative control reactions were performed in the absence of either the enzyme or the substrate. It was ensured that auxiliary enzymes were not rate limiting. One unit (1 U) of enzyme activity is defined as 1 µmol substrate consumed or product formed per minute.

Bioinformatic analysis

Crystal structures were obtained from the Protein Data Bank (PDB), and structural models were retrieved from the AlphaFold Protein Structure Database (version 3.0) (22). Structural analyses and comparative assessments were performed using UCSF ChimeraX (41). Amino acid sequences for alignment were retrieved from UniProt, and multiple sequence alignments were generated using the EMBL-EBI Job Dispatcher framework (24), followed by manual refinement and editing in BioEdit.

Data availability

All study data are included in the article and SI Appendix. In addition, the kinetic data and model simulations are available as Excel files and Mathematica notebooks on the FAIRDOMHub (*https://fairdomhub.org/investigations/775*) and will be made public upon publication of the manuscript.

Acknowledgements

This study was supported by grants from and the German Science Foundation (DFG Gu1522/2-2, Gu1522/5-1, SI 642/14-1, SI 642/14-2, FOR2816, GRK2749/1). We acknowledge financial assistance from the DSI/NRF in South Africa (grant NRF-SARCHI 82813 to J. L. S.). We thank Markus Brand, Frauke Caliebe, Friederike Hörsch, Carolin Kremer and Maria Patti for engaged discussions.

Additional information

Author's contributions

RO, MT, RF, AM, MB, and CP, performed the experiments; MB, CB, JLS, BS, KG supervised, RO, MT, RF, AM, MB, CP, CB, JLS, MH, BS, and KG analyzed data; RO, AM, and KG wrote the original draft; all authors wrote, reviewed, and edited; BS, and KG conceptualized the study; BS and KG acquired funding.

Declaration of generative AI and AI-assisted technologies in the manuscript preparation process

During the preparation of this work the author(s) used ChatGPT (Open AI 2025), ChatGPT Team (5.1) and DeepL in order to optimize language. After using this tool/service, the authors reviewed and edited the content as needed and take full responsibility for the content of the published article.

Funding

Funder	Grant reference number	Author
Deutsche Forschungsgemeinschaft (DFG)	SI 642/14-2	Ravi Shakar Ojha
Deutsche Forschungsgemeinschaft (DFG)	Gu1522/2-2	Marius Theune
Deutsche Forschungsgemeinschaft (DFG)	GRK2749/1	Ruben Fritsche
Deutsche Forschungsgemeinschaft (DFG)	Gu1522/5-1	Alexander Makowka
Deutsche Forschungsgemeinschaft (DFG)	SI 642/14-1	Carmen Peraglie
DSI/NRF in South Africa	NRF-SARCHI 82813	Jacky L Snoep
Deutsche Forschungsgemeinschaft (DFG)	FOR2816	Martin Hagemann

Author ORCID iDs

Kirstin Gutekunst: https://orcid.org/0000-0003-4366-423X

Additional files

Supplementary information

References

1. **Chen X.**, et al. (2016) The Entner–Doudoroff pathway is an overlooked glycolytic route in cyanobacteria and plants. *Proceedings of the National Academy of Sciences* **113**:5441-5446 https://doi.org/10.1073/pnas.1521916113 | PubMed

2. **Evans S. E.,** et al. (2024) Plastid ancestors lacked a complete Entner-Doudoroff pathway, limiting plants to glycolysis and the pentose phosphate pathway. *Nature Communications* **15**:1102 https://doi.org/10.1038/s41467-024-45384-y | PubMed

3. **Schulze D.,** et al. (2022) GC/MS-based 13C metabolic flux analysis resolves the parallel and cyclic photomixotrophic metabolism of Synechocystis sp. PCC 6803 and selected deletion mutants including the Entner-Doudoroff and phosphoketolase pathways. *Microbial Cell Factories* **21**:69 https://doi.org/10.1186/s12934-022-01790-9 | PubMed

4. **Makowka A.,** et al. (2020) Glycolytic Shunts Replenish the Calvin–Benson–Bassham Cycle as Anaplerotic Reactions in Cyanobacteria. *Molecular Plant* **13**:471-482 https://doi.org/10.1016/j.molp.2020.02.002 | PubMed

5. **Lucius S.,** Makowka A., Michl K., Gutekunst K., Hagemann M. (2021) The Entner-Doudoroff Pathway Contributes to Glycogen Breakdown During High to Low CO2 Shifts in the Cyanobacterium Synechocystis sp. PCC 6803. *Frontiers in Plant Science* **12**:787943 https://doi.org/10.3389/fpls.2021.787943 | PubMed

6. **Koch M.,** Doello S., Gutekunst K., Forchhammer K. (2019) PHB is Produced from Glycogen Turn-over during Nitrogen Starvation in Synechocystis sp. PCC 6803. *International Journal of Molecular Sciences* **20**:1942 https://doi.org/10.3390/ijms20081942 | PubMed

7. **Doello S.,** Klotz A., Makowka A., Gutekunst K., Forchhammer K. (2018) A specific glycogen mobilization strategy enables awakening of dormant cyanobacteria from chlorosis. *Plant Physiology* **177**:594-603 https://doi.org/10.1104/pp.18.00297 | PubMed

8. **Kim S.,** Lee S. B. (2006) Catalytic Promiscuity in Dihydroxy-Acid Dehydratase from the Thermoacidophilic Archaeon Sulfolobus solfataricus. *Journal of Biochemistry* **13G**:591-596 https://doi.org/10.1093/jb/mvj057 | PubMed

9. **d M.,** Muñoz-Marín C., López-Lozano A., Moreno-Cabezuelo J. Á., Díez J., García-Fernández J. M. (2024) Mixotrophy in cyanobacteria. *Current Opinion in Microbiology* **78**:102432 https://doi.org/10.1016/j.mib.2024.102432 | PubMed

10. **Gupta R. D.** (2016) Recent advances in enzyme promiscuity. *Sustainable Chemical Processes* **4**:2 https://doi.org/10.1186/s40508-016-0046-9

11. **Gupta M. N.,** Uversky V. N. (2023) Moonlighting enzymes: when cellular context defines specificity. *Cell Mol Life Sci* **80**:130 https://doi.org/10.1007/s00018-023-04781-0 | PubMed

12. **Xie N.,** Sharma C., Rusche K., Wang X. (2024) Phosphoketolase and KDPG aldolase metabolisms modulate photosynthetic carbon yield in cyanobacteria. *The Plant cell* https://doi.org/10.1093/plcell/koae291 | PubMed

13. **Zhang P.,** et al. (2020) Cyanobacterial Dihydroxyacid Dehydratases Are a Promising Growth Inhibition Target. *ACS Chemical Biology* **15**:2281-2288 https://doi.org/10.1021/acschembio.0c00507 | PubMed

14. **Matsubara K.,** et al. (2014) One-step synthesis of 2-keto-3-deoxy-d-gluconate by biocatalytic dehydration of d-gluconate. *J Biotechnol* **1G1**:69-77 https://doi.org/10.1016/j.jbiotec.2014.06.005 | PubMed

15. **Carsten J. M.,** Schmidt A., Sieber V. (2015) Characterization of recombinantly expressed dihydroxy-acid dehydratase from Sulfobus solfataricus-A key enzyme for the conversion of carbohydrates into chemicals. *J Biotechnol* **211**:31-41 https://doi.org/10.1016/j.jbiotec.2015.06.384 | PubMed

16. **Wolterink-van Loo S.,** et al. (2007) Biochemical and structural exploration of the catalytic capacity of Sulfolobus KDG aldolases. *Biochem J* **403**:421-430 https://doi.org/10.1042/bj20061419 | PubMed

17. **Oubrie A.,** Rozeboom H. J., Dijkstra B. W. (1999) Active-site structure of the soluble quinoprotein glucose dehydrogenase complexed with methylhydrazine: A covalent cofactor-inhibitor complex. *Proceedings of the National Academy of Sciences* **G6**:11787-11791 https://doi.org/10.1073/pnas.96.21.11787 | PubMed

18. **Wu X.-Y.,** Ding H.-T., Ke L.-P., Xin Y.-Y., Cheng X. (2012) Characterization of an acid-resistant glucose 1-dehydrogenase from Bacillus cereus var. mycoides. *Roumanian biotechnological letters* **17**:7540-7548

19. **Miao R.,** Jahn M., Shabestary K., Peltier G., Hudson E. P. (2023) CRISPR interference screens reveal growth-robustness tradeoffs in Synechocystis sp. PCC 6803 across growth conditions. *Plant Cell* **35**:3937-3956 https://doi.org/10.1093/plcell/koad208 | PubMed

20. **Lee J.-M.,** et al. (2005) Identification of a glucokinase that generates a major glucose phosphorylation activity in the cyanobacterium Synechocystis sp. PCC C803. *Mol Cells* **19**:256-261 PubMed

21. **Theune M. L.,** et al. (2021) In-vivo quantification of electron flow through photosystem I – Cyclic electron transport makes up about 35% in a cyanobacterium. *Biochimica et Biophysica Acta (BBA) - Bioenergetics* **1862**:148353 https://doi.org/10.1016/j.bbabio.2020.148353 | PubMed

22. **Abramson J.,** et al. (2024) Accurate structure prediction of biomolecular interactions with AlphaFold 3. *Nature* **630**:493-500 https://doi.org/10.1038/s41586-024-07487-w | PubMed

23. **Walters M. J.,** et al. (2008) Characterization and crystal structure of Escherichia coli KDPGal aldolase. *Bioorg Med Chem* **16**:710-720 https://doi.org/10.1016/j.bmc.2007.10.043 | PubMed

24. **Madeira F.,** et al. (2024) The EMBL-EBI Job Dispatcher sequence analysis tools framework in 2024. *Nucleic Acids Res* **52**:W521-w525 https://doi.org/10.1093/nar/gkae241 | PubMed

25. **Wymer N.,** et al. (2001) Directed Evolution of a New Catalytic Site in 2-Keto-3-Deoxy-6-Phosphogluconate Aldolase from Escherichia coli. *Structure* **G**:1-9 https://doi.org/10.1016/s0969-2126(00)00555-4 | PubMed

26. **Allard J.,** Grochulski P., Sygusch J. (2001) Covalent intermediate trapped in 2-keto-3-deoxy-6-phosphogluconate (KDPG) aldolase structure at 1.95-angstrom resolution. *Proceedings of the National Academy of Sciences of the United States of America* **G8**:3679-3684 https://doi.org/10.1073/pnas.071380898 | PubMed

27. **Bachhar A.,** Jablonsky J. (2022) Entner-Doudoroff pathway in Synechocystis PCC 6803: Proposed regulatory roles and enzyme multifunctionalities. *Front Microbiol* **13**:967545 https://doi.org/10.3389/fmicb.2022.967545 | PubMed

28. **Hauenstein J.,** et al. (2026) BRENDA in 2026: a Global Core Biodata Resource for functional enzyme and metabolic data within the DSMZ Digital Diversity. *Nucleic Acids Res* **54**:D527-d534 https://doi.org/10.1093/nar/gkaf1113 | PubMed

29. **Ahmed H.,** et al. (2005) The semi-phosphorylative Entner-Doudoroff pathway in hyperthermophilic archaea: a re-evaluation. *Biochem J* **3G0**:529-540 https://doi.org/10.1042/bj20041711 | PubMed

30. **Fabris M.,** et al. (2012) The metabolic blueprint of Phaeodactylum tricornutum reveals a eukaryotic Entner–Doudoroff glycolytic pathway. *The Plant Journal* **70**:1004-1014 https://doi.org/10.1111/j.1365-313x.2012.04941.x | PubMed

31. **Chauton M. S.,** Winge P., Brembu T., Vadstein O., Bones A. M. (2012) Gene Regulation of Carbon Fixation, Storage, and Utilization in the Diatom Phaeodactylum tricornutum Acclimated to Light/Dark Cycles. *Plant Physiology* **161**:1034-1048 https://doi.org/10.1104/pp.112.206177 | PubMed

32. **Kennedy F.,** Martin A., Bowman J. P., Wilson R., McMinn A. (2019) Dark metabolism: a molecular insight into how the Antarctic sea-ice diatom Fragilariopsis cylindrus survives long-term darkness. *New Phytologist* **223**:675-691 https://doi.org/10.1111/nph.15843 | PubMed

33. **Bräsen C.,** Esser D., Rauch B., Siebers B. (2014) Carbohydrate Metabolism in Archaea: Current Insights into Unusual Enzymes and Pathways and Their Regulation. *Microbiology and Molecular Biology Reviews* **78**:89 https://doi.org/10.1128/mmbr.00041-13 | PubMed

34. **Lorentzen E.,** Siebers B., Hensel R., Pohl E. (2005) Mechanism of the Schiff base forming fructose-1,6-bisphosphate aldolase: structural analysis of reaction intermediates. *Biochemistry* **44**:4222-4229 https://doi.org/10.1021/bi048192o | PubMed

35. **Bradford M. M.** (1976) A rapid and sensitive method for the quantitation of microgram quantities of protein utilizing the principle of protein-dye binding. *Analytical Biochemistry* **72**:248-254 https://doi.org/10.1016/0003-2697(76)90527-3 | PubMed

36. **Fullerton S. W.,** et al. (2006) Mechanism of the Class I KDPG aldolase. *Bioorg Med Chem* **14**:3002-3010 https://doi.org/10.1016/j.bmc.2005.12.022 | PubMed

37. **Edelheit O.,** Hanukoglu A., Hanukoglu I. (2009) Simple and efficient site-directed mutagenesis using two single-primer reactions in parallel to generate mutants for protein structure-function studies. *BMC Biotechnol* **G**:61 https://doi.org/10.1186/1472-6750-9-61 | PubMed

38. **Zor T.,** Selinger Z. (1996) Linearization of the Bradford protein assay increases its sensitivity: theoretical and experimental studies. *Anal Biochem* **236**:302-308 https://doi.org/10.1006/abio.1996.0171 | PubMed

39. **Buchanan C. L.,** Connaris H., Danson M. J., Reeve C. D., Hough D. W. (1999) An extremely thermostable aldolase from Sulfolobus solfataricus with specificity for non-phosphorylated substrates. *Biochem J* **343**:563-570 https://doi.org/10.1042/bj3430563 | PubMed

40. **Krevet S.,** et al. (2020) Enzymatic Synthesis of 2-Keto-3-Deoxy-6-Phosphogluconate by the 6-Phosphogluconate-Dehydratase From Caulobacter crescentus. *Frontiers in Bioengineering and Biotechnology* **8** https://doi.org/10.3389/fbioe.2020.00185 | PubMed

41. **Pettersen E. F.,** et al. (2021) UCSF ChimeraX: Structure visualization for researchers, educators, and developers. *Protein Sci* **30**:70-82 https://doi.org/10.1002/pro.3943 | PubMed

Peer reviews

Reviewer #1 (Public review):

Summary:

Some of the authors proposed in a PNAS paper in 2016 the occurrence of the Entner-Doudoroff (ED) pathway in cyanobacteria and plants, on the basis of several lines of biochemical and genetic evidence. However, more recent results indicated that one of the two specific enzymes of the ED pathway (EDD) is missing in Synechocystis PCC 6803. The authors carried out additional experiments, which demonstrated that EDD is missing, and one of the enzymes (ED aldolase) is a promiscuous enzyme which seems to be involved in proline metabolism and is not actually participating in the ED pathway as initially believed. The results described in this paper are strong evidence that this new interpretation is appropriate, and therefore, it corrects the previous proposal, providing an honest description of the reasons why the authors had reached the wrong conclusion about the existence of the ED pathway in cyanobacteria and plants.

Strengths:

Thorough reanalysis of the experimental results obtained in previous studies, which led to the publication of the PNAS paper in 2016.

New experimental evidence to confirm that enzymes previously considered as participating in the ED actually are not catalyzing the ED biochemical reactions, but are involved in other metabolic pathways. Also, the authors completely discarded the occurrence of the GDH/GK shunt in Synechocystis PCC 6803. Generally speaking, the manuscript is very clearly written, with a precise description of the previous findings, the mistakes which took place in the 2016 paper, and the strategies they have used to address those issues, in order to reach a thoroughly revised vision of the glucose metabolic pathways in Synechocystis PCC 6803. In this regard, the drawings shown in Figures 1 and 7 are very helpful for the reader to follow the story and understand the possible metabolic transformations depending on the working hypothesis.

Also, I commend the authors for openly describing previous mistakes. In this paper, they reassess past observations in light of more recent findings and to integrate the information in this manuscript. The scientific conclusions are solid and very interesting, and besides, they use the opportunity to offer valuable advice to researchers. This is especially focused on the importance of careful biochemical characterization of enzymes, which should always be carried out when studying proteins which have been identified as a specific enzyme on the basis of sequence homology. In a similar way, they found that an insertional mutant was the cause of the absence of specific metabolites, which had been attributed to particularities of a metabolic pathway in that mutant, when it was actually due to a nucleotide insertion; this could have been easily prevented by confirming the correct generation of the mutant by DNA sequencing.

Weaknesses:

The authors propose that EDA might be involved in the PEP-pyruvate-OAA node, or in the proline metabolism, but this requires further experimental work for clarification; what their results indicate clearly is that this enzyme is not actually catalyzing the transformation of KDPG to GAP, which is the second specific enzyme of the ED pathway. But the real physiological function in this cyanobacterium is still unconfirmed.

Another aspect which could be improved is that the recombinant expression of some genes was carried out in E. coli; even if this is a useful and valid research strategy, in studies like this (where there is a strong focus on the physiological function of enzymes in the original organism, Synechocystis PCC 6803), I think it would have been more appropriate to express the 6803 genes in another cyanobacterium easily amenable for genetic transformation and gene expression, which would produce the protein in a physiological environment more similar to another cyanobacterium (compared to E. coli, which is an heterotrophic bacterium). I am not sure this would change any of the obtained results, but it certainly would confer additional robustness to the enzymatic results.

Bibliography:

I think the list of papers used in this manuscript is complete and up to date. However, I do miss recent papers which addressed one aspect that was proposed in the original 2016 PNAS paper: the authors wrote, "We therefore suggest that Prochlorococcus might oxidize glucose via the ED pathway under mixotrophic conditions, as shown for Synechocystis." Recent studies checked this hypothesis and have shown that the ED pathway seems to be also missing in Prochlorococcus and marine Synechococcus, and I think this manuscript is a good place to cite them, since these results are consistent with the findings of this paper.

https://doi.org/10.7554/eLife.111485.1.sa2

Reviewer #2 (Public review):

Summary:

The study presents novel results on the presence of the Entner-Doudoroff pathway in Synechocystis sp. PCC 6803. In contrast to an earlier study, compelling evidence is given that this strain lacks both an ED pathway and a glucose dehydrogenase/glucokinase bypass but contains a promiscuous aldolase, which also decarboxylates oxaloacetate and cleaves 2-keto-4-hydroxyglutarate (as it occurs in proline degradation). The study concludes with successfully reconciling data from different studies and with lessons learned from the previous misconception.

Strengths:

Solid biochemical data are presented to reconcile contradicting data of earlier studies and to serve as a basis for disclosing possible functions of a promiscuous aldolase. Earlier misconceptions and lessons to be learned are well discussed.

Weaknesses:

The materials and methods section is rather lengthy, suffering from a lack of conciseness and repetition, and nevertheless misses some specifications.

https://doi.org/10.7554/eLife.111485.1.sa1

Author response:

> ***Reviewer #1 (Public review):***
>
> *Summary:*
>
> *Some of the authors proposed in a PNAS paper in 2016 the occurrence of the Entner-Doudoroff (ED) pathway in cyanobacteria and plants, on the basis of several lines of biochemical and genetic evidence. However, more recent results indicated that one of the two specific enzymes of the ED pathway (EDD) is missing in Synechocystis PCC 6803. The authors carried out additional experiments, which demonstrated that EDD is missing, and one of the enzymes (ED aldolase) is a promiscuous enzyme which seems to be involved in proline metabolism and is not actually participating in the ED pathway as initially believed. The results described in this paper are strong evidence that this new interpretation is appropriate, and therefore, it corrects the previous proposal, providing an honest description of the reasons why the authors had reached the wrong conclusion about the existence of the ED pathway in cyanobacteria and plants.*

We thank Reviewer 1 for the summary and comments. We found that EDA is a promiscuous aldolase that, in addition to the cleavage of KDPG to GAP and pyruvate (a reaction of the ED pathway) catalyzes other reactions *in vitro*. Based on the *in vitro* results obtained, potential *in vivo* functions of EDA are proposed, including its involvement in proline metabolism. However, these assumptions require further experimental testing. We do not yet have definitive findings regarding the function of the promiscuous aldolase EDA in *Synechocystis in vivo*, but respective studies are currently underway.

> *Strengths:*
>
> *Thorough reanalysis of the experimental results obtained in previous studies, which led to the publication of the PNAS paper in 2016.*
>
> *New experimental evidence to confirm that enzymes previously considered as participating in the ED actually are not catalyzing the ED biochemical reactions, but are involved in other metabolic pathways. Also, the authors completely discarded the occurrence of the GDH/GK shunt in Synechocystis PCC 6803. Generally speaking, the manuscript is very clearly written, with a precise description of the previous findings, the mistakes which took place in the 2016 paper, and the strategies they have used to address those issues, in order to reach a thoroughly revised vision of the glucose metabolic pathways in Synechocystis PCC 6803. In this regard, the drawings shown in Figures 1 and 7 are very helpful for the reader to follow the story and understand the possible metabolic transformations depending on the working hypothesis.*
>
> *Also, I commend the authors for openly describing previous mistakes. In this paper, they reassess past observations in light of more recent findings and to integrate the information in this manuscript. The scientific conclusions are solid and very interesting, and besides, they use the opportunity to offer valuable advice to researchers.*

> *This is especially focused on the importance of careful biochemical characterization of enzymes, which should always be carried out when studying proteins which have been identified as a specific enzyme on the basis of sequence homology. In a similar way, they found that an insertional mutant was the cause of the absence of specific metabolites, which had been attributed to particularities of a metabolic pathway in that mutant, when it was actually due to a nucleotide insertion; this could have been easily prevented by confirming the correct generation of the mutant by DNA sequencing.*

We agree that biochemical characterization of enzymes as well as DNA sequencing to check deletion mutants, are important and valuable tools. As outlined in the manuscript and additionally in more detail in a recently submitted article, which is available at bioRxiv (Theune et al. 2026, doi: *https://doi.org/10.64898/2026.04.08.717167*) and is currently under review at PLOS One, we suggest that genome sequencing of deletion mutants in combination with complemented strains as controls are required to minimize the risk of misinterpretation based on secondary mutations (1). During the early stages of our research on the ED pathway, and later as well when we were already trying to resolve the conflicting results that had accumulated concerning the ED pathway, genome sequencing for *Synechocystis* mutants was not affordable as a routine procedure (2-4). Therefore, we could not have easily prevented this misconception based on this technique at that time. However, we strongly encourage genome sequencing of deletion mutants in combination with complemented strains as routine procedures these days (1).

> *Weaknesses:*
>
> *The authors propose that EDA might be involved in the PEP-pyruvate-OAA node, or in the proline metabolism, but this requires further experimental work for clarification; what their results indicate clearly is that this enzyme is not actually catalyzing the transformation of KDPG to GAP, which is the second specific enzyme of the ED pathway. But the real physiological function in this cyanobacterium is still unconfirmed.*

As stated above and in the manuscript, we agree that the *in vivo* role of EDA requires further experimental work which is in progress. However, our results demonstrate that EDA splits KDPG into GAP and pyruvate *in vitro*, but we assume that this reaction does not play a role *in vivo* due to the absence of its substrate.

> *Another aspect which could be improved is that the recombinant expression of some genes was carried out in E. coli; even if this is a useful and valid research strategy, in studies like this (where there is a strong focus on the physiological function of enzymes in the original organism, Synechocystis PCC 6803), I think it would have been more appropriate to express the 6803 genes in another cyanobacterium easily amenable for genetic transformation and gene expression, which would produce the protein in a physiological environment more similar to another cyanobacterium (compared to E. coli, which is an heterotrophic bacterium). I am not sure this would change any of the obtained results, but it certainly would confer additional robustness to the enzymatic results.*

Synechocystis is easily amendable to genetic manipulation, and we agree that expression and purification of all enzymes from this host would have been ideal. However, the first characterization of *Synechocystis* EDA was performed with proteins that were purified from *Synechocystis* and showed activity on KDPG at comparable rates as proteins that were purified from *E. coli* in this study (2). Moreover, most biochemical characterizations of EDAs from archaea, bacteria and plants were performed after recombinant expression in *E. coli* and yielded highly active enzyme as in the case of *Synechocystis* is this study (5-7). Therefore, we currently have no reason to worry that the expression in *E. coli* might affect the enzymatic activity of EDA. The main reason for utilizing *E. coli* as an expression strain in this study was to gain higher yields of protein for in-depth analyses.

> *Bibliography:*
>
> *I think the list of papers used in this manuscript is complete and up to date. However, I do miss recent papers which addressed one aspect that was proposed in the original 2016 PNAS paper: the authors wrote, "We therefore suggest that Prochlorococcus might oxidize glucose via the ED pathway under mixotrophic conditions, as shown for Synechocystis." Recent studies checked this hypothesis and have shown that the ED pathway seems to be also missing in Prochlorococcus and marine Synechococcus, and I think this manuscript is a good place to cite them, since these results are consistent with the findings of this paper.*

We will include a references from Moreno-Cabezuelo et a. 2023 (DOI: 10.1128/spectrum.03275-22) in which the proteomes of three marine *Prochlorococcus* and three marine *Synechococcus* strains were investigated upon exposure to glucose (8). Protein levels of EDA were either downregulated or not affected while proteins involved in OPP pathway and CBB cycle were upregulated. The authors of this study conclude that this indicates that the latter processes rather than the ED pathway are involved in photomixotrophy in these strains. However, flux analyses are still missing.

> ***Reviewer #2 (Public review):***
>
> *Summary:*
>
> *The study presents novel results on the presence of the Entner-Doudoroff pathway in Synechocystis sp. PCC 6803. In contrast to an earlier study, compelling evidence is given that this strain lacks both an ED pathway and a glucose dehydrogenase/glucokinase bypass but contains a promiscuous aldolase, which also decarboxylates oxaloacetate and cleaves 2-keto-4-hydroxyglutarate (as it occurs in proline degradation). The study concludes with successfully reconciling data from different studies and with lessons learned from the previous misconception.*
>
> *Strengths:*
>
> *Solid biochemical data are presented to reconcile contradicting data of earlier studies and to serve as a basis for disclosing possible functions of a promiscuous aldolase. Earlier misconceptions and lessons to be learned are well discussed.*
>
> *Weaknesses:*
>
> *The materials and methods section is rather lengthy, suffering from a lack of conciseness and repetition, and nevertheless misses some specifications.*

We thank Reviewer 2 for the summary and comments and will improve the materials and methods part accordingly in a revised version.

(1) M. Theune et al., Easy-to-use whole-genome sequencing workflows and standardized practices to uncover hidden genetic variation in Synechocystis PCC 6803 wild-type and knock-out strains. bioRxiv 10.64898/2026.04.08.717167, 2026.2004.2008.717167 (2026).

(2) X. Chen et al., The Entner–Doudoroff pathway is an overlooked glycolytic route in cyanobacteria and plants. Proceedings of the National Academy of Sciences 113, 5441-5446 (2016).

(3) D. Schulze et al., GC/MS-based 13C metabolic flux analysis resolves the parallel and cyclic photomixotrophic metabolism of Synechocystis sp. PCC 6803 and selected deletion mutants including the Entner-Doudoroff and phosphoketolase pathways. Microbial Cell Factories 21, 69 (2022).

(4) A. Makowka et al., Glycolytic Shunts Replenish the Calvin–Benson–Bassham Cycle as Anaplerotic Reactions in Cyanobacteria. Molecular Plant 13, 471-482 (2020).

https://doi.org/10.7554/eLife.111485.1.sa0